

25

NASA Contractor Report 2906

Use of Sensitivity Analysis
to Predict Pilot Performance as
a Function of Different Displays

Michael L. Mout, George H. Burgin,
and Michael J. Walsh

CONTRACT NAS1-14416
NOVEMBER 1977

NASA

NASA Contractor Report 2906

Use of Sensitivity Analysis
to Predict Pilot Performance as
a Function of Different Displays

Michael L. Mout, George H. Burgin,
and Michael J. Walsh
Decision Science, Inc.
San Diego, California

Prepared for
Langley Research Center
under Contract NAS1-14416



National Aeronautics
and Space Administration

Scientific and Technical
Information Office

1977

Page Intentionally Left Blank

PREFACE

The work reported herein was authorized under Contract NAS1-14416. Preliminary, closely-related work was performed under Contract NAS1-13734. Both studies were conducted under the direction of Patrick Gainer, Simulation and Human Factors Branch, Langley Research Center.

This study was performed at Decision Science, Inc., San Diego, with Michael L. Mout acting as principal investigator. George H. Burgin and Michael J. Walsh contributed to the computational implementation of the Kalman filter.

The original idea of evaluating displays by sensitivity analysis was conceived by Patrick Gainer and is documented in the Langley Research Center working paper No. 1131, "A Method of Analyzing and Evaluating Visual Displays."

Page Intentionally Left Blank

CONTENTS

	Page
SUMMARY	1
INTRODUCTION	2
GLOSSARY	3
SYMBOLS	6
BACKGROUND	8
Static Model	10
Summary	10
Mathematical Model	11
Computer Program for Static Display Evaluation	12
Results of a Simple Experiment and the Static Display Technique	13
Summary of the Results	14
Experimental Conclusion	14
Kalman Filter	14
Mathematical Model	16
Kalman Filter and the Static Model	21
Look-Point Controller	25
Mathematical Models	25
1) Local minimum-weighted trace	25
2) Minimum-weighted trace-limited look points	26
3) Weighted mini-max with limited look points	27
Final Model Formulation	28
COMPUTER PROGRAM	29
Display Setup	29
Kalman Filter Options and Parameters	30
Look-Point Controller Options and Parameters	31
Program Output	33
ANALYTICAL RUNS	34
ILS FLight Situation	34
Description of Display Setup	34

	Page
Pilot Tasks--Automatic and Manual Approach	34
Results of Computer Simulations	35
Fixed Look Points	35
Variance Weight and System Noise	37
Automatic Approach	38
Manual Approach	40
AREAS OF FURTHER INVESTIGATION	41
Time Step	41
Variance Weights	41
System Noise (Variance)	42
Display Modification	42
Closed-Loop Controller	42
REFERENCES	43
APPENDIX A (Derivation of Simplified Forms of the Gain Matrix)	44
APPENDIX B (Glide Slope Indicator (GSI) Response)	46
FIGURES	47
TABLES	72

USE OF SENSITIVITY ANALYSIS TO PREDICT PILOT
PERFORMANCE AS A FUNCTION OF DIFFERENT DISPLAYS

By Michael L. Mout, George H. Burgin, and Michael J. Walsh
Decision Science, Inc.

SUMMARY

This report describes a novel technique for computer simulation and evaluation of visual displays as they relate to human scanning behavior and control performance. A computer program has been written for a general situation, but the usage in this report is specifically for pilot performance in aircraft control.

The computer program sets up some general flight situation with a given set of displays. A look-point controller simulates visual scanning of these displays. It does this by picking a look point at each time step that minimizes some estimation error criterion. The result of each run is a covariance matrix of state variable estimation for each point in time during the simulation. This covariance matrix gives two types of measures. One is the variance, or standard deviation, measure for each state variable. This measure indicates the accuracy with which that state variable can be estimated with the display setup being considered and the present look point. Other values derived from the covariance matrix are the correlations between state variables. These correlations are a measure of the complexity of the display setup with respect to the present look point.

Several runs were made simulating an Instrument Landing System (ILS) approach. Runs with user-controlled (fixed) look points generated error measures and complexity measures that

seem to be intuitively correct. Runs with the look-point controller resulted in scanning patterns similar to human behavior. These patterns were noted for both automatic and manual ILS approaches.

INTRODUCTION

The derivation of visual information about an aircraft state from a display or set of displays can be a complex process. Figure 1 is a simplified flow chart of this process. The human observer must know or be able to approximate how the display responds to changes in the various state variables. He needs some measure of how accurately he is able to estimate the changes in the displays themselves. He must know the amount of inherent noise in either the state variables and/or the display system. He must also know how the state and control variables are related in time. With this information, the pilot/observer has the capability of estimating the changes in the aircraft's state variables and the accuracy of that estimation. He uses this information to derive control inputs which allow him to extrapolate to the next state. The next state estimate is used to control the display look point for the next time step.*

The purpose of this investigation was to develop a digital computer program for dynamic display evaluation and scanning simulation. This program was to be used for evaluation of possible pilot performance on conceptually designed display setups prior to actual hardware construction of these displays. This program is based on a static display evaluation technique (Reference 1) derived by Patrick Gainer. This static technique

*The simulation in this report is done in discrete time steps (such as, 1/16 second or 1/8 second). For the sake of brevity, any future references to "time" in this report will imply "time step."

has been incorporated into a computer program using Kalman filter techniques to generate dynamic display/flight motion and a visual scanning simulation.

The scanning simulation is accomplished by a look-point controller which minimizes some user-defined error criterion. This controller allows the user to define weights for the various state variables then select look points by minimizing either the weighted mini-max estimation error or the weighted covariance matrix trace (sum of the weighted variances). This minimization is either through an iteration process for a local minimum or over a small set of predetermined look points.

This program is presently set up to simulate seven standard cockpit instruments under ILS conditions. The program has been written to allow for any general display setup and can be modified for a variety of flight conditions and display/state relationships.

GLOSSARY

Altimeter:	Altitude indicator display.
Command Bars:	(Vertical and Horizontal) Displays showing the best control commands to retain the glide slope path.
Control Vector:	Values for control of the future state vector values.
Correlation:	Measure (ranges from -1 to +1) of how two variables change with respect to one another.
Display Segments:	Arbitrary segments into which each display is divided.
Display Weights:	Overall weights for each display indicating general degradation of visual

acuity of that display. Can be specified for the total simulation and for each new read-in look point.

Eight Ball: Artificial horizon display showing roll, pitch, and sometimes yaw.

Glideslope: Landing approach descent path which will result in ideal landing conditions.

Glideslope Indicator (GSI): Display showing the vertical angular distance above or below the glideslope.

Influence Matrix: Matrix giving the influence of changes in the state vector to changes in the display segments.

Look Point Location in display set where the observer looks for one time step.

Look-Point Controller: Computer algorithm that controls the look point for the next time step.

Look-Point Controller Weights: Weights for each state variable used by the look-point controller algorithm in the minimization criterion. These weights are related to the relative size of the state variable standard deviations and their relative importance to the pilot/observer.

Segment Weights: Values for each segment indicating the relative amount of information in that segment.

Variance of Estimation: A measure of the amount of expected error in estimating the value of a variable.

Vertical Speed Indicator (VSI): Display showing the rate of change of altitude.

Visual Acuity
(position or rate):

A measure of the accuracy with which an observer can perceive change of position location or change of rate of movement of a display segment. A decrease in the acuity measure indicates a decrease in the accuracy of measurement. The inverse of the acuity measure is the standard deviation of the error of estimation.

SYMBOLS

A_i	Matrix relating present time, i , state variables to next time, $i+1$, state variables.
$ac(\lambda)$	Acuity measure for a polar angle λ .
B_i	Matrix relating present time, i , control variables to next time, $i+1$, state variables.
cb_h, cb_v	Horizontal (cb_h) and vertical (cb_v) control commands displayed by the <u>command bars</u> .
cr_i	Optimization criterion for the look-point controller algorithm.
D_i	Matrix relating present time, i , system (or turbulence) noise to future time, $i+1$, state variables.
$fa(j, k, \ell; \underline{x})$ $fb(j, k, \ell; \underline{x})$	Display/state functions relating the state vector \underline{x} to the location ($fa =$ horizontal, $fb =$ vertical) of segment j, k in display ℓ .
I	Identity matrix.
K_i	Gain matrix from Kalman Filter. Measure of the weight given to the observations and to the observation covariance matrix, Ξ_i in estimating the present and future state vectors, $\hat{\underline{x}}_{i i}$ and $\hat{\underline{x}}_{i+1 i}$.

m_0	Expected value of the initial state, \underline{x} .
nv	Number of state variables.
\underline{o}_i	Vector of observations at time i ; two observations per segment, one for horizontal displacement, and one for vertical displacement.
$tr(\Sigma)$	Trace of matrix Σ , sum of diagonal values.
\underline{u}_i	Control vector at i^{th} time step.
W	Diagonal matrix of controller weights' with state variable weights on diagonal.
\underline{x}_i	State vector at time i . For ILS simulations, $\underline{x}' = (\psi, \theta, \phi, x_r, y_r, z_r, \dot{x}_r, \dot{y}_r, \dot{z}_r, cb_h, cb_v)$.
$\hat{\underline{x}}_i i$	Estimate of state vector at time i based on the observations at times $i, i-1, i-2 \dots, 1, \text{ and } 0$.
$\hat{\underline{x}}_{i+1 i}$	Estimate of the state vector at time $i+1$ based on observation $i, i-1, i-2, \dots, 1, \text{ and } 0$.
x_r, y_r, z_r	Runway fixed coordinates x_r = range to end of runway y_r = distance off-line of the runway z_r = altitude above runway
$\dot{x}_r, \dot{y}_r, \dot{z}_r$	Rate of change of x_r, y_r, z_r
$\alpha_{jkl}, \alpha_{jkl}$	Longitudinal and latitudinal coordinates of segment j, k in display ℓ .

\underline{x}_i	State vector noise (turbulence) at time i .
Γ_i	Covariance matrix of state vector noise, time i .
$\frac{\partial fa[fb]}{\partial x_m}(j, k, \ell; \underline{x})$	Partial derivative of horizontal [vertical = fb] display state function with respect to the m^{th} state variable. $m = 1, nv$.
$\lambda_{\alpha_i}, \lambda_{\beta_i}$	Longitudinal and latitudinal coordinates of the look angle at time i .
$\lambda_i(j, k, \ell)$	Polar angle from look point at time i to center of segment j, k , display ℓ .
$\underline{\xi}_i$	Observation error time step i .
Ξ_i	Covariance matrix of observation error at time i .
$\Sigma_{i i}$	Covariance matrix of the error of the state vector estimation $\hat{\underline{x}}_{i i}$.
$\Sigma_{i+1 i}$	Covariance matrix of the error in $\hat{\underline{x}}_{i+1 i}$.
T_i	Influence matrix at time, i . Consists of partial derivations of fa and fb with respect to \underline{x}_i . Relates display segment changes to changes in the state variables, \underline{x}_i .
ψ, θ, ϕ	Euler angles, yaw, pitch, and roll

BACKGROUND

The original idea for a mathematical algorithm for evaluation of a visual display was put forth in 1973 by Patrick Gainer in Langley Working Paper LWP1131. In 1974

a contract was awarded by Langley Research Center (LRC) to Decision Science, Inc. (DSI) to design a computer program to implement this static display evaluation technique (Reference 1 contains a description of this work).

This computer program was valid for displays which did not move and for fixed look points. A simple experiment was conducted at the DSI facility that verified the results of the program. Several problems were noted that made it difficult to apply this initial program to any real-life display situations. The basic problem was the inability to incorporate movement of the displays into the program.

The static technique does not include additional information that is available to an aircraft pilot. The location of the display segments, the display/state relationship, and the pilot's look point are all the information that is accounted for in the static program; see the area in Figure 1 enclosed in dotted lines. In real life, the pilot has additional knowledge of the time history of the aircraft movement and the effect of the present state and the present control inputs on the future aircraft state. Also, the pilot has some knowledge of the amount of noise (turbulence) he can expect in the state variables.

A second contract was awarded to DSI in 1975 to expand the original static technique and program to include dynamic display evaluation and to also include a look-point controller algorithm which could, in a sense, simulate the pilot's visual scanning behavior.

The Kalman Filter provided much promise for the dynamic extension of the static technique. Several look-point controllers were to be analyzed as possible candidates for simulating human scanning.

Static Model

Summary.- The static model is based on two assumptions. The first assumption is that a display can be divided into arbitrarily small segments as in Figure 2. The second assumption is that for small changes in the state variables these segments can be considered to have only horizontal and vertical change (no rotation).

For example, in Figure 2 the display is shown in a zero position in the top figure with the initial segmentation. The middle figure shows a pitch down change. This causes a positive change in each segment's latitudinal location ($\Delta\beta > 0$). The bottom figure shows a negative pitch and positive roll. This causes changes in each segment's location. The segment shown has a positive change in longitude ($\Delta\alpha > 0$) and a negative change in latitude ($\Delta\beta < 0$).

Based on the above assumptions an equation can be derived for estimating the state vector from the observation of the horizontal and vertical displacement of the display segments. The accuracy of this estimation is dependent on the accuracy of observation of these displacements. This accuracy is assumed to be dependent on the polar angle between each segment's center point and the observer's fixation point as in the top figure, Figure 2. This angle determines the acuity of that center point, and the inverse of the acuity squared is the variance of this observation.

For example, in Figure 2 the top figure shows a fixation point located at λ_α longitude and λ_β latitude angle from the display center. Each segment has an angle associated with this look point. Segment number 4 has an angle from the look point of $\lambda(4)$, segment 2 has an angle of $\lambda(2)$. Each segment's angle to the look point is used to determine an acuity

value (see Figure 3 for a sample acuity function). In this case, the acuity for segment 4, $ac[\lambda(4)]$, will be larger than $ac[\lambda(2)]$. This means that less error will be experienced in estimating change in position of segment 4 than for change in segment 2.

The variances of the display segment observations are used in the derivation of the covariance matrix of estimation of the state vector. This covariance matrix is used to evaluate various look points within a display and compare the relative worth of various displays or display setups.

For example, in the top figure, Figure 2, fixation point two is better than point one because the associated estimation covariance matrix has smaller values both on and off the diagonal. This means that with the second fixation point less state variable (pitch and roll) estimation error will be incurred, and there will be less confusion between changes of pitch and roll as compared to fixation point one.

Mathematical Model.- Let the state vector be represented by \underline{x} , $\underline{x}' = (x_1, x_2, x_3 \dots, x_{nv})$. The display is divided into m horizontal segments and n vertical segments, making $n \times m$ total segments with α_{ij} , β_{ij} being the longitudinal and latitudinal angles of the i, j^{th} segment. Let

$$fa_{ij} = fa(\alpha_{ij}, \beta_{ij}; \underline{x})$$

$$fb_{ij} = fb(\alpha_{ij}, \beta_{ij}; \underline{x})$$

be the functions that relate values of the state vector to values of α_{ij} and β_{ij} , respectively.

Now the influence matrix, so called because it determines how the state variables influence the display variables, can be defined as (see following page).

$$T = \begin{Bmatrix} \frac{\partial f_{a_{11}}}{\partial x_1}, \frac{\partial f_{a_{11}}}{\partial x_2} \dots, \frac{\partial f_{a_{11}}}{\partial x_{nv}} \\ \frac{\partial f_{b_{11}}}{\partial x_1}, \frac{\partial f_{b_{11}}}{\partial x_2} \dots, \frac{\partial f_{b_{11}}}{\partial x_{nv}} \\ \vdots \\ \frac{\partial f_{a_{nm}}}{\partial x_1}, \frac{\partial f_{a_{nm}}}{\partial x_2} \dots, \frac{\partial f_{a_{nm}}}{\partial x_{nv}} \\ \frac{\partial f_{b_{nm}}}{\partial x_1}, \frac{\partial f_{b_{nm}}}{\partial x_2} \dots, \frac{\partial f_{b_{nm}}}{\partial x_{nv}} \end{Bmatrix}$$

So if the observation vector, \underline{o} , is defined as the vector of changes of each segment in horizontal and vertical direction, then

$$\underline{o} = T \cdot \underline{x}.$$

The covariance matrix of the estimates of these observations, $\text{cov}(\hat{\underline{o}})$, is a diagonal matrix with the inverse of the square of each segment's acuity on the diagonal. It can be shown (Reference 1) that the estimate of the state variable, $\hat{\underline{x}}$, is

$$\hat{\underline{x}} = [T' \text{cov}(\hat{\underline{o}})^{-1} T]^{-1} T' \text{cov}(\hat{\underline{o}})^{-1} \hat{\underline{o}}$$

It follows that the covariance of this estimate reduces to

$$\text{cov}(\hat{\underline{x}}) = [T' \text{cov}(\hat{\underline{o}})^{-1} T]^{-1}.$$

This is basically the technique the static computer program implements. A more detailed discussion of these equations can be found in Reference 1.

Computer Program for Static Display Evaluation.-The computer program for static display evaluation was written in as general a form as possible. This allowed the user to create a wide variety of display setups with many display/state

variable functions. Various user specified input parameters were used to allow the user to establish the number of state variables, number of displays, size and segmentation of each display, various input and printout options, a variety of display/state functions, and position or rate of movement for the acuity functions. The program was written to allow the user to modify or add FORTRAN subroutines for new display/state functions or different acuity functions.

The program was exercised on a wide variety of displays and look points. The results of these runs agreed with intuition as regards the values in the covariance matrices.

The program was modified to allow weighting of different displays to indicate sequential look points, but this was not a satisfactory solution for the dynamic display situation.

Results of a Simple Experiment and the Static Display Technique.-A simple experiment was devised and conducted at the DSI facility. This experiment was designed to verify the Static Display Evaluation technique by comparing the theoretical covariance matrices calculated by the program with the actual experimental sample covariance matrix.

The experiment was designed to generate a series of state variable estimations for each of several look points. The observer was instructed to fixate on a certain spot, then line up a movable cross hairs with a fixed cross hairs. The accuracy of the final location of the movable cross hairs was used to calculate a state variable estimate of yaw, pitch, and roll.

The same look points and a display model were read into the computer program. The total experiment is reported in Reference 1.

Summary of the Results.- The theoretical covariance matrices were calculated for two different weighting schemes on all four experimental conditions. The first weighting scheme was a gross approximation of the actual display and resulted in theoretical variances which were much lower than the sample variances. The second weighting scheme was an attempt to more precisely reflect the actual display. This scheme resulted in much larger theoretical variance values. The values were, in most cases, not significantly different from the sample variances. Under both weighting schemes most of the sample correlations were not significantly different from the theoretical.

Experimental Conclusion.- The primary conclusion to be drawn from these results is that the basic computer model of the display can drastically effect the analysis. When using the proper setup, the algorithm seems to be a valid model of human performance. There are many consistencies noted between the sample covariance matrices and the theoretical matrices. The presence of the consistencies gives a strong indication that further experimental data would be valuable for a more in-depth verification of this model.

Kalman Filter

The Kalman Filter is based on a process that has linearly, time-related state and control variables, and system noise or turbulence, with known probability distribution. These state variables are linearly related to observation variables, which have estimation errors with known probability distribution.

A Kalman Filter is a computational algorithm to provide estimates about a state vector at a time t_i , given an estimate of the state vector at time t_{i-1} (and all previous times, $t_{i-2} \dots t_0$) and an observation vector at time t_i . The Kalman Filter was originally described by Kalman in References

2 and 3; a concise summary of the technique and its computational aspects may be found in Reference 4.

If we denote the true state vector at time t_i with \underline{x}_i and its estimate by $\hat{\underline{x}}_{i|i}$, the Kalman Filter provides a recursive algorithm by which $\hat{\underline{x}}_{i|i}$ can be determined so that $E[(\hat{\underline{x}}_{i|i} - \underline{x}_i)(\hat{\underline{x}}_{i|i} - \underline{x}_i)]$ is minimized. Therefore, $\hat{\underline{x}}_{i|i}$ is a best estimate in the least squares sense.

The Kalman Filter obtains $\hat{\underline{x}}_{i|i}$ in two steps. In a first step, it calculates a predicted estimate of the state vector at time t_i ($\hat{\underline{x}}_{i|i-1}$) from the estimate of the state vector at the preceding time ($\hat{\underline{x}}_{i-1|i-1}$) and its covariance matrix $\Sigma_{i-1|i-1}$ and the (given) state transition matrix and control vector. For the calculation of these quantities, the observations at time t_i are not yet used.

In an intermediate step, a weighting or gain matrix is calculated. This gain matrix is a function of the system under observation, and for its calculation the covariance matrix of the predicted estimate of the state vector as well as those transformations describing the system under observation are used.

The second step of the Kalman filtering process now takes into account the observations made at time t_i . First, an observation vector ($\hat{\underline{o}}_i$) which would correspond to the predicted estimate of the state vector, is calculated. The actual observations made at time t_i (\underline{o}_i) will, in general, be different from these predicted observations and the difference ($\hat{\underline{o}}_i - \underline{o}_i$) is formed. The final estimate of the state vector is then a linear combination of the predicted estimate and the weighted (by the gain matrix) difference ($\hat{\underline{o}}_i - \underline{o}_i$). The covariance matrix of the final estimate may be obtained at the same time as the gain matrix is calculated because it is a function of the same variables.

For example, Figure 4 shows a simple process to which Kalman Filter techniques may be applied. In this example a dot has controlled movement in a plane. At time zero, the dot is near (1, 1). A control value of (-1, -1) is input at times 0 and 1. This makes the dot move close to (0, 0) at time 1 and (-1, -1) at time 2. The control at time 2 is (-1, 0). This moves the dot to approximately (-2, -1) at time 3. The noise in this movement perturbs the actual location as seen in the figure.

The observation of this dot's movement is on a linear scale that shows the sum of the coordinates of the dot at each time step along with nonzero random noise. At time zero, the observation is at +2.55. This is the sum of the zeroth coordinates (1.2, .85) plus a random noise value of .5.

At time 1, the observation is $-.05 = .25 - .05$ [$-.25$ (random noise)]. The random noise at times 2 and 3 is .25 and $-.1$ giving observation values of -1.57 and -3.10 , respectively.

Here, the state, control, and noise variables (x , y , u_x , u_y , γ_x , and γ_y , respectively) are related linearly in time by

$$x_{i+1} = x_i + u_{x_i} + \gamma_{x_i}$$

$$y_{i+1} = y_i + u_{y_i} + \gamma_{y_i}$$

Also, the observation variable (o) is linearly related to the state variables and the random noise (ξ) by

$$o_i = x_i + y_i + \xi_i$$

Mathematical Model.- The process to which Kalman Filter techniques apply has a general formulation. Specifically, if we let \underline{x}_i be the state vector at time step i , then

$$\underline{x}_{i+1} = A_i \underline{x}_i + B_i \underline{u}_i + D_i \underline{\gamma}_i$$

where

$$\underline{x}_0 = \underline{m}_0 + D_0 \underline{y}_0$$

$$\underline{u}_i = \text{Control Vector}$$

A_i , B_i , and D_i = Matrices relating the present state and the control and noise vectors to the next state.

and

$$\underline{m}_0 = \text{Expected value of } \underline{x}_0$$

$$\Gamma_i = \text{Covariance matrix of the state vector noise, } \gamma_i.$$

Also, if \underline{o}_i is the observation vector, then

$$\underline{o}_i = T_i \underline{x}_i + \xi_i$$

where

$$T_i = \text{Matrix relating state vector, } \underline{x}_i, \text{ to the observation, } \underline{o}_i.$$

and

$$\Xi_i = \text{Covariance matrix of the observation error, } \xi_i.$$

In the example, Figure 4,

$$\underline{x}'_i = (\underline{x}_i, y_i); \underline{u}'_i = (u_{x_i}, u_{y_i})$$

$$A_i = B_i = D_i = I = \begin{Bmatrix} 1 & 0 \\ 0 & 1 \end{Bmatrix}; \underline{m}'_0 = (1, 1)$$

$$\Gamma_i = \begin{Bmatrix} .015 & 0 \\ 0 & .015 \end{Bmatrix}$$

and

$$T_i = (1, 1)$$

$$\Xi_i = .4.$$

Many analytical results have been derived for the Kalman Filter. Specifically, least squares estimates for the present state vector, $\hat{x}_i|i$ and the next state vector, $\hat{x}_{i+1|i}$, have been formulated. Also, the corresponding covariance matrices ($\Sigma_i|i+1, \Sigma_i|i$) of these estimates are available along with the gain matrix, K_i . These are as follows:

$$\hat{x}_{i+1|i} = A_i \hat{x}_i|i + B_i u_i$$

$$\Sigma_{i+1|i} = A_i' \Sigma_i|i A_i + D_i \Gamma_i D_i$$

and

$$\hat{x}_i|i = \hat{x}_i|i-1 + K_i [O_i - T_i' \hat{x}_i|i-1].$$

Also, the gain matrix, K_i , is found as

$$K_i = \Sigma_i|i-1 T_i' [T_i \Sigma_i|i-1 T_i' + \Xi_i]^{-1}.$$

Finally,

$$\Sigma_i|i = [I - K_i \cdot T_i] \Sigma_i|i-1$$

The initial conditions are given as

$$\hat{x}_0 = \underline{m}_0 = E(x_0) = \text{The expected value of } x_0$$

and

$$\Sigma_{0|0} = \text{Initial given covariance matrix.}$$

(See Reference 2 for the derivation of these estimates.)

As shown in Appendix A, K_i can be reduced further to

$$K_i = \Sigma_i|i T_i \Xi_i^{-1}$$

with

$$\Sigma_{i|i} = \left[\Sigma_{i|i-1}^{-1} + T_i' \Sigma_i^{-1} T_i \right]^{-1}.$$

The latter form of K_i is more desirable in this application as it requires the inversion of a much smaller dimensioned matrix than the initial form.

Referring to the example in Figure 4 with $\Sigma_{0|0}$ given as

$$\Sigma_{0|0} = \begin{pmatrix} 1 & 0 \\ 0 & 1 \end{pmatrix}$$

and

$$\hat{x}'_{0|0} = \underline{m}'_0 = (1, 1).$$

so that

$$\hat{x}_{1|0} = \begin{pmatrix} 1 & 0 \\ 0 & 1 \end{pmatrix} \begin{pmatrix} 1 \\ 1 \end{pmatrix} + \begin{pmatrix} 1 & 0 \\ 0 & 1 \end{pmatrix} \begin{pmatrix} -1 \\ -1 \end{pmatrix} = \begin{pmatrix} 0 \\ 0 \end{pmatrix}$$

and

$$\begin{aligned} \Sigma_{1|0} &= \begin{pmatrix} A'_0 & \Sigma'_{0|0} & A_0 \\ D'_0 & \Gamma_0 & D_0 \end{pmatrix} \\ &= \begin{pmatrix} 1 & 0 \\ 0 & 1 \end{pmatrix} \begin{pmatrix} 1 & 0 \\ 0 & 1 \end{pmatrix} \begin{pmatrix} 1 & 0 \\ 0 & 1 \end{pmatrix} + \begin{pmatrix} 1 & 0 \\ 0 & 1 \end{pmatrix} \begin{pmatrix} .015 & 0 \\ 0 & .015 \end{pmatrix} \begin{pmatrix} 1 & 0 \\ 0 & 1 \end{pmatrix} \\ &= \begin{pmatrix} 1.015 & 0 \\ 0 & 1.015 \end{pmatrix}. \end{aligned}$$

It should be noted that in this example the observation space is one dimensional and the state space is two dimensional. This does not invalidate this process for the Kalman Filter technique since there is assumed knowledge of Σ_0 and \underline{m}_0 . With this process the covariance matrix $\Sigma_{i|i}$ will converge to a singular matrix as $i \rightarrow \infty$.

Now for time 1

$$\begin{aligned}\Sigma_{1|1} &= \left[\begin{matrix} [\Sigma_{1|0}]^{-1} & & \\ & T_1^T & \Sigma_1^{-1} & T_1 \\ & & & \end{matrix} \right]^{-1} \\ &= \left[\begin{pmatrix} 1.015 & 0 \\ 0 & 1.015 \end{pmatrix}^{-1} + \begin{pmatrix} 1 \\ 1 \end{pmatrix} (.4)^{-1} (1 \ 1) \right]^{-1} \\ &= \left[\begin{pmatrix} .9852 & 0 \\ 0 & .9852 \end{pmatrix} + \begin{pmatrix} 2.5 & 2.5 \\ 2.5 & 2.5 \end{pmatrix} \right]^{-1} \\ &= \begin{pmatrix} 3.49 & 2.5 \\ 2.5 & 3.49 \end{pmatrix}^{-1} = \begin{pmatrix} .591 & -.4234 \\ -.4234 & .591 \end{pmatrix}\end{aligned}$$

$$K_1 = \begin{pmatrix} .591 & -.4234 \\ -.4234 & .591 \end{pmatrix} \begin{pmatrix} 1 \\ 1 \end{pmatrix} (.4)^{-1} = \begin{pmatrix} .419 \\ .419 \end{pmatrix}$$

and

$$\begin{aligned}\hat{x}_{1|1} &= \begin{pmatrix} 0 \\ 0 \end{pmatrix} + \begin{pmatrix} .419 \\ .419 \end{pmatrix} - \begin{bmatrix} 0.5 & - (1 \ 1) \end{bmatrix} \begin{pmatrix} 0 \\ 0 \end{pmatrix} \\ &= \begin{pmatrix} 0 \\ 0 \end{pmatrix} + \begin{pmatrix} -.021 \\ -.021 \end{pmatrix} = \begin{pmatrix} -.021 \\ -.021 \end{pmatrix}.\end{aligned}$$

Following this process for the remaining time steps:

time = 2

$$\Sigma_{2|1} = \begin{pmatrix} .606 & -.4234 \\ -.4234 & .606 \end{pmatrix}$$

$$\hat{x}_{2|1} = \begin{pmatrix} -1.021 \\ -1.021 \end{pmatrix}$$

$$\Sigma_{2|2} = \begin{pmatrix} .5624 & -.4670 \\ -.4670 & .5624 \end{pmatrix}$$

$$K_2 = \begin{pmatrix} .2385 \\ .2385 \end{pmatrix}$$

$$\hat{x}_{2|2} = \begin{pmatrix} -.908 \\ -.908 \end{pmatrix}$$

time 3

$$\Sigma_{3|2} = \begin{pmatrix} .5774 & -.4670 \\ -.4670 & .5774 \end{pmatrix}$$

$$\hat{x}_{3|2} = \begin{pmatrix} -1.908 \\ -.908 \end{pmatrix}$$

$$\Sigma_{3|3} = \begin{pmatrix} .2391 & -.2154 \\ -.2154 & .2391 \end{pmatrix}$$

$$K_3 = \begin{pmatrix} .0592 \\ .0592 \end{pmatrix} \text{ and } \hat{x}_{3|3} = \begin{pmatrix} -1.925 \\ -.925 \end{pmatrix}$$

It can be seen in this example that the covariance matrix of the present estimate ($\Sigma_{i|i}$) is decreasing as i increases and that it is tending to converge to some matrix that is determined by the matrices r , r , and Ξ . Also, the covariance matrix of the prediction ($\Sigma_{i+1|i}$) is larger than $\Sigma_{i|i}$ by a constant value of .015 on the diagonal. The corresponding state estimates are within the bounds established by the covariance matrices.

Kalman Filter and the Static Model.- The relation between the Kalman Filter and the static model is in the observation equation. In the previously described equations the same variable names, matrix names, and notation were used in the Kalman Filter observation equation as in the static model. This makes the final step that brings the static model together with the dynamic Kalman Filter method more clear. To make this step, note that the cov (\hat{O}) in the static discussion is the matrix Ξ_i in the Kalman Filter. Thus, the observation error $\underline{\epsilon}_i$ becomes the error due to the lack of the acuity for the look point at the time step i . In other words, the matrix Ξ_i is a diagonal matrix with dimension equal to twice the number of display segments. If we let

$ac(\lambda)$ = acuity of a segment that has a polar angle of λ degrees from the look point.

Also let

$\lambda_i(j, k, \ell)$ = angle between the i^{th} look point and segment j, k in display ℓ .

time step. In more complex displays this matrix, Ξ_i , could change drastically with each time step depending upon the amount of change in the look point during each time step.

The remaining adaptations of the Kalman Filter for dynamic display evaluation are in the state vector equations. Here, the control vector, its relationship to the next state, the size of the state vector noise, and the relation between present and future states can be adapted to approximate the flight conditions or vehicle conditions under consideration.

For example, the sample runs shown later in this report simulate a landing descent with nine state variables,

$$\underline{x}' = (\psi, \theta, \phi, x_r, y_r, z_r, \dot{x}_r, \dot{y}_r, \dot{z}_r)$$

with no significant movement in yaw, ψ ; roll, ϕ ; distance off course, y_r ; or \dot{y}_r . Here.

$$\underline{m}'_0 = (0^\circ, -2.5^\circ, 0^\circ, -10,770 \text{ meters}, 0 \text{ m.}, 460 \text{ m.}, 85 \text{ m. per second}, 0, -3.7 \text{ m. per second});$$

that is, the initial conditions are -2.5° pitch down from level flight (2.5° glide slope), 10,770 meters from the end of the runway, altitude of 460 meters, speed 85 meters per second (165 knots), and descent rate 230 meters per minute.

The transition matrix, A_i , for time steps of one eighth of a second is

$$A_i = \begin{matrix} & \psi & \theta & \phi & x_r & y_r & z_r & \dot{x}_r & \dot{y}_r & \dot{z}_r \\ \begin{matrix} \psi \\ \theta \\ \phi \\ x_r \\ y_r \\ z_r \\ \dot{x}_r \\ \dot{y}_r \\ \dot{z}_r \end{matrix} & \left\{ \begin{array}{cccccccc} 1 & 0 & 0 & 0 & 0 & 0 & 0 & 0 & 0 \\ 0 & 1 & 0 & 0 & 0 & 0 & 0 & 0 & 0 \\ 0 & 0 & 1 & 0 & 0 & 0 & 0 & 0 & 0 \\ 0 & 0 & 0 & 1 & 0 & 0 & 1/8 & 0 & 0 \\ 0 & 0 & 0 & 0 & 1 & 0 & 0 & 1/8 & 0 \\ 0 & 0 & 0 & 0 & 0 & 1 & 0 & 0 & 1/8 \\ 0 & 0 & 0 & 0 & 0 & 0 & 1 & 0 & 0 \\ 0 & 0 & 0 & 0 & 0 & 0 & 0 & 1 & 0 \\ 0 & 0 & 0 & 0 & 0 & 0 & 0 & 0 & 1 \end{array} \right. \end{matrix}$$

For 1/16 second time steps, the \dot{x}_r , \dot{y}_r , and \dot{z}_r column and x_r , y_r , and z_r row values would be 1/16 instead of 1/8.

The control vector for this simulation run corrects θ , z_r , and \dot{x}_r . The control function corrects θ to -2.5° , adjusts z_r to be on the 2.5° glide slope (see Appendix B), and keeps \dot{x}_r at 85 meters per second (165 knots).

$$\underline{u}' = \theta_{\text{control}}, z_{\text{control}}, \dot{x}_{\text{control}}$$

so that the control matrix, B, has the form

$$B = \begin{matrix} \psi \\ \theta \\ \phi \\ x_r \\ y_r \\ z_r \\ \dot{x}_r \\ \dot{y}_r \\ \dot{z}_r \end{matrix} \begin{Bmatrix} 0 & 0 & 0 \\ 1 & 0 & 0 \\ 0 & 0 & 0 \\ 0 & 0 & 0 \\ 0 & 0 & 0 \\ 0 & 1 & 0 \\ 0 & 0 & 1 \\ 0 & 0 & 0 \\ 0 & 0 & 0 \end{Bmatrix}$$

For this example, the noise vector contains values for each state variable, and the D matrix is the identity matrix. Also, for 1/8 second time step

$$\sigma_\psi = \sigma_\phi = \sigma_{y_r} = \sigma_{\dot{y}_r} = 0$$

$$\sigma_\theta = 2.0 \text{ min. of arc per } 1/8 \text{ second}$$

$$\sigma_{x_r} = 1.5 \text{ meters per } 1/8 \text{ second}$$

$$\sigma_{z_r} = .077 \text{ meters per } 1/8 \text{ second}$$

$$\sigma_{\dot{x}_r} = .015 \text{ meters per } 1/8 \text{ second}^2 = .03 \text{ knots per } 1/8 \text{ sec.}$$

$$\sigma_{\dot{z}_r} = .185 \text{ meters per minute per } 1/8 \text{ sec.} = .003 \text{ meters per } 1/8 \text{ sec.}^2$$

so that

$$E = \begin{Bmatrix} 0 & 0 & 0 & \cdot & \cdot & \cdot & \cdot & 0 & 0 \\ 0 & 2. & 0 & \cdot & \cdot & \cdot & \cdot & \cdot & \cdot \\ 0 & 0 & 0 & 0 & \cdot & \cdot & \cdot & \cdot & \cdot \\ \cdot & \cdot & 0 & 5 & 0 & \cdot & \cdot & \cdot & \cdot \\ \cdot & \cdot & 0 & 0 & 0 & 0 & \cdot & \cdot & \cdot \\ \cdot & \cdot & \cdot & \cdot & 0 & .25 & 0 & \cdot & \cdot \\ \cdot & \cdot & \cdot & \cdot & 0 & 0 & .05 & 0 & \cdot \\ 0 & \cdot & \cdot & \cdot & \cdot & \cdot & 0 & 0 & 0 \\ 0 & \cdot & \cdot & \cdot & \cdot & \cdot & \cdot & 0 & .01 \end{Bmatrix}$$

Look-Point Controller

The final step in developing the dynamic display evaluation was to incorporate a method or methods which could be combined with the Kalman Filter to control the look point for each time step. These look-point controllers would minimize some error criterion through the use of the statistics generated from the Kalman Filter. The use of this controller would result in performance measures over time that could possibly be used as a minimum base line ("best") for human pilot performance. In other words, if the acuity function, system noise, and all other parameters correctly reflect the real-life or pilot-simulator situation, then the perfect human pilot should be able to achieve performance comparable to that predicted by the program.

Mathematical Models.- Three look-point controllers have been incorporated into the system:

1) Local minimum-weighted trace

This controller calculates the covariance matrix for the next time step at the present look point. This is called the zeroth candidate look point for time $i+1$. The covariance matrix for this look point is

$$\Sigma_{i+1|i+1}^0 = [\Sigma_{i+1|i}^{-1} + T'_{i+1} \Xi_{i+1}^{-1} T_{i+1}]^{-1}$$

The trace of this matrix is taken as the zeroth criterion at time i

$$cr_{i+1}^0 = \text{tr}(\Sigma_{i+1|i+1}^0).$$

Now four look points are chosen equidistant from the present look point (these will usually be the centers of four adjacent display segments). The covariance matrix is calculated for each of these look points along with the trace. This gives cr_{i+1}^1 , cr_{i+1}^2 , cr_{i+1}^3 , and cr_{i+1}^4 . If any of these values are

smaller than cr_{i+1}^0 , then cr_{i+1}^0 is set equal to that value, and the associated look point is taken as a new zeroth candidate look point for time $i+1$. This process continues until a candidate look point is found such that

$$cr_{i+1}^0 \leq cr_{i+1}^j \text{ for } j = 1, 2, 3, 4.$$

This look point satisfies the local minimum on $\text{tr}(\Sigma_{i+1}|_{i+1})$.

This model can also use the minimizable criterion of the weighted trace, where

$$cr_{i+1}^0 = \text{tr}(\Sigma_{i+1}^0|_{i+1}W)$$

where W is a diagonal matrix with weights for the various state variable variances on the diagonal.

2) Minimum-weighted trace-limited look points

The first method is a thorough method designed to find the best look point in the total display setup. The only problem with this scheme is that it can consume large amounts of computer time since it may look at a large number of points before arriving at a minimum. This is especially true in a complex display set. Also, it does not imitate human behavior in that it may well choose look points between displays. This would be in order to get information from two or more displays at once. Human visual behavior tends to concentrate on one display at a time.

With these ideas in mind, the algorithm was modified to limit the candidate look points to one point in each display, such as the center of each display as follows:

Assume there are n displays and let

$\text{long}_\ell, \text{lat}_\ell =$ longitudinal and latitudinal coordinates of the center of the ℓ^{th} display.

Now calculate $cr_{i+1}^\ell, \ell = 1, 2, 3 \dots, n$

with

$$cr_{i+1}^{\ell} = \text{tr}(\Sigma_{i+1|i+1}^{\ell} W)$$

as before except that the associated look points will be long_{ℓ} , and lat_{ℓ} . If

$$cr_{i+1}^j \leq cr_{i+1}^{\ell} \text{ for all } \ell,$$

then choose the look point associated with display j as the $(i+1)^{\text{st}}$ look point.

This algorithm intuitively would seem more likely to generate scanning patterns more similar to human pilot scanning than the first algorithm. With this technique, the next look point should go to the display associated with the variable whose weighted variance is disproportionately larger than the other variables; otherwise, the look point would stay on a central display.

3) Weighted mini-max with limited look points

In this technique, the previous algorithm was adapted to a different error criterion. In this case, the algorithm picks the maximum weighted diagonal element of the covariance matrix of the next state prediction ($\Sigma_{i+1|i} W$), then minimizes that value in $\Sigma_{i+1|i+1}$. So that if σ_k^2 is any diagonal element of $\Sigma_{i+1|i}$ and w_k is the k^{th} diagonal element of the weight matrix, W , then find j such that

$$w_j \sigma_j^2 \geq w_k \sigma_k^2 \text{ for all } k = 1, 2, 3 \dots, nv$$

The algorithm now searches for the display look point that minimizes the σ_j^2 in $\Sigma_{i+1|i+1}$. In other words, $cr_{i+1}^{\ell} = \sigma_j^2$.

These diagonal values are the variances of the state variables. So, if the weighted variance of a state variable is large in $\Sigma_{i+1|i}$, then the look point for time step $i+1$ should be in a display that is associated with that variable.

This algorithm seems to more intuitively reflect the human pilot's behavior than the previous two algorithms. Here, it is presumed that the pilot only looks at a particular display when he feels his estimate of the variable or variables associated with that display are being estimated more inaccurately, in a weighted sense, than the other variables.

For example, assume there are three state variables with three separate displays, one for each variable. Assume that at time step i

$$\Sigma_{i+1|i} = \begin{Bmatrix} 5.0 & 3.2 & 4.6 \\ 3.2 & 10 & 3.0 \\ 4.6 & 3.0 & 7 \end{Bmatrix}$$

and

$$W = \begin{Bmatrix} 2.1 & 0 & 0 \\ 0 & 1.0 & 0 \\ 0 & 0 & 1.6 \end{Bmatrix}$$

so that

$$cr_{i+1}^1 = \sigma_1^2 \cdot W_1 = 10.5$$

$$cr_{i+1}^2 = \sigma_2^2 \cdot W_2 = 10$$

$$cr_{i+1}^3 = \sigma_3^2 \cdot W_3 = 11.2.$$

Therefore, the $i+1^{st}$ look point should be the display associated with the third variable.

Final Model Formulation

The final model uses the static display setup and evaluation with the dynamic Kalman Filter movement to create a simulation of a set of moving displays. Using this simulation with the look-point controller results in scan patterns similar to the scan of a human observer of a set of moving displays.

These patterns and the associated statistics can be used to evaluate a display set with respect to effective human use.

The general formulation of the model can be seen in the flow chart in Figure 5A. At point A, all of the simulation setup has been decided upon, and the simulated time begins with some predetermined look point. At each time step, the model generates a new state vector and observation vector according to the Kalman Filter parameters and the present look point. Using these values, the model then derives the present Kalman Filter results and the predicted results. This information is used by the look-point controller to determine the next look point. This procedure continues until the desired simulation time has elapsed. Figure 5B gives a flowchart of the Kalman Filter process.

COMPUTER PROGRAM

The flow chart in Figure 5A gives a brief description of how this technique works. A more complete flow chart is shown in Figure 6. This flow chart more accurately describes how the computer program actually implements the method. Here, the program user first reads in the display setup; this includes the various size, weighting, locations, and function options. Next the dynamic process (Kalman Filter) options are read in. These options describe the type of flight conditions that will be simulated. Finally, the look-point controller options and weights are read in. Once the options and parameters are determined the program begins the simulation for the required time period. Once the simulation is completed, the program looks for a new simulation if it is desired; if not, the computer run is completed.

Display Setup

Figure 7, Flow Chart A, shows how and when the display parameters and option are established. Up to seven displays

can be specified in the program. Each display is separately described in terms of location, size, and display segmentation. Also, a variety of display types can be specified. These include, but are not limited to, horizontal or vertical linear display, circular dial display, eight ball or artificial horizon display, T.V. camera or artificial runway display, and glide-slope indicator. Display types that are not included can be incorporated into the program with a user-provided subroutine. The display parameters can specify the state variables to be displayed, proportional movement, and various other values.

The final display option, which is treated separately, is the segment weights. These weights usually range from zero to one, cannot be negative, and indicate the amount of relative information in each segment under initial simulation conditions. These weights can be reset every time step, after a read-in look point of $\lambda_{\alpha} = 1000$, or set and left at all ones. The display setup and weighting determine the values of the influence matrix, T , which relate display movement to state vector changes.

Kalman Filter Options and Parameters

Figure 8, Flow Chart B, demonstrates the selection of the read-in parameters and options for the Kalman Filter dynamic display portion of the computer program. The first values read in concerning the Kalman Filter are the option for reading the A, B, and D matrices (ABDOPT) and the option for reading or calculating the control vector \underline{u} (CNTRLOP). The ABDOPT value allows for reading the A, B, and D matrices initially only, or reading in new matrices at each time step. The CNTRLOP value determines if the control vector is only read in initially, read in each time step, or calculated at each time step in a subroutine called UCALC.

Next to be read is the number of time steps (the size of

each time step is determined by the A, B, and D matrices). The initial state vector values, $\underline{m}_0 = E(\underline{x}_0)$, are read in next, after which follows the system noise (state vector standard deviations) parameters. These noise values and the D matrix determine the amount of random change that occurs in the state vector from one time step to the next. The last values that concern the Kalman Filter are the A, B, and D matrices and the control vector. These are read in or calculated according to the ABDOPT and CNTRLOP values.

As stated earlier, the Kalman Filter calculates \underline{x}_{i+1} , such that

$$\underline{x}_{i+1} = A_i \underline{x}_i + B_i \underline{u}_i + D_i \gamma_i$$

where

$$\text{cov}(\underline{\gamma}_i) = \Gamma = \text{diagonal matrix with } \sigma_{\gamma_j}^2 \text{ on the diagonal}$$

and

$$\sigma_{\gamma_j} = \text{standard deviation of system noise or turbulence of state variable } j.$$

So that matrix A determines what effect the present state, \underline{x}_i , has in one time step on the next state, \underline{x}_{i+1} . The B matrix determines how the present control vector, \underline{u}_i , effects the state vector in one time step. Finally, the D matrix determines the effect of the system noise, $\underline{\gamma}_i$, in one time step on the state vector, \underline{x}_{i+1} .

Look-Point Controller Options and Parameters

There are five look-point controller options. The value LKOPT determines which of several algorithms are used for finding the look point for the next time step. The five look-point controller options are as follows:

1. Use the last read-in look point, no calculations involved. The program does not operate the look-point controller subroutine until a look point has been read in with a negative degradation factor. With option 1, this last look point is used as a constant for the remainder of the simulation run.

2. Calculate center of weighted segments. This option should be used when only one display or possibly two adjacent displays are being simulated. Under this option the look point control calculates the location of the center of the weighted segments and chooses that location as the next look point. Previous experiences with the static technique indicated that this is an approximate optimum look point for one display.

3. Local minimum weighted trace ($\text{tr}[\Sigma_{i+1|i+1}W]$). Using the numerical iterative technique described earlier this option finds a look point that is a local minimum of the sum of weighted diagonal values of the covariance matrix of the next look point, $\Sigma_{i+1|i+1}$.

4. Minimum of all displays of the weighted trace of $\Sigma_{i+1|i+1}$ ($\text{tr}[\Sigma_{i+1|i+1}W]$). In this option the weighted trace of $\Sigma_{i+1|i+1}$ is calculated for one look point in each display. The look point with the smallest value is selected.

5. Weighted mini-max. Minimize, over all displays, variance of variable with maximum predicted weighted variance. Using this option, the controller finds the largest diagonal element of the weighted predicted covariance matrix ($\Sigma_{i+1|i}W$). $\Sigma_{i+1|i}$ is based on the present look point. The program then calculates the covariance matrix for a look point in each display. The look point is chosen which minimizes the diagonal value of $\Sigma_{i+1|i+1}$ previously determined to be maximum for $\Sigma_{i+1|i}W$.

Program Output

The program contains several output options along with a standard output at each time step. Figure 9 shows a flow chart of the printed output. The program will initially print the program title along with the various options and parameters that have been chosen. This may be followed by an optional printout of the influence matrix, τ . This influence matrix printout will occur periodically, if chosen, throughout the simulation run. The influence matrix is recalculated only after a significant change in the state vector and will be printed when recalculated.

The next printout to occur will be the weighted values of the segments for each display. This is only if and when the weights are read in. If the weights are all set to one, there will be no printout. The look point for the next or initial step is now printed. The location of this look point with respect to each display is given and the manner in which it was determined; that is, whether or not the look point was read in or calculated and how it was calculated is printed out.

Following the look-point print is an optional printout of the display observation values. These values are the horizontal and vertical displacements (printed separately) of each segment of each display. These are the changes due to change in the state vector in the past time step (step $i-1$ to i).

The final printout occurs with each time step (nonoptional). It includes the present time step, present estimation of the state vector change in last time step, the actual state vector values, the covariance matrix of the estimation, and the corresponding correlation matrix with standard deviations on the diagonal. This same printout is generated for the predicted change from time i to time $i+1$. The A, B, and D matrices are printed at this time also, if they are being changed or initialized. The same is true of the print of the control vector, \underline{u}_i .

ANALYTICAL RUNS

ILS Flight Situation.- The Instrument Landing Situation (ILS) is the most critical portion of flight control. Because of this, many ILS simulators are available along with data from experiments using the simulators; therefore, an ILS approach was decided upon as the first area of investigation using the dynamic display evaluation program.

For simplicity's sake, several assumptions have been made which were deemed not to affect the situation under study; that is, the viewing of the active displays under ILS conditions. The assumptions are that the aircraft is on course and is stable in roll and yaw. The sources of turbulence (system noise) are due to pitch, range to go (x_r), altitude (z_r), \dot{x}_r , and \dot{z}_r . The aircraft is assumed to be perfectly controlled; in other words, any departure from the ideal flight path is corrected at the next time step. When in use, the command bars are considered as separate state variables.

Description of Display Setup.- Figure 10 shows a mock-up of the various active displays. These are the eight ball, glide slope indicator, altimeter, vertical speed indicator, airspeed indicator, and the vertical and horizontal command bars. The response of the various displays to changes in the state variables is obvious, except for possibly the command bars and the glide slope indicator. In this case, when active, the command bars display the command state variables in a one-to-one fashion. The glide slope indicator (GSI) shows deviations from a 2.5° glide slope up to $\pm 1.8^\circ$. This is determined by the range to go, x_r , and altitude, z_r (see Appendix B, GSI response).

Pilot Tasks--Automatic and Manual Approach.- Two tasks are being compared in this investigation. One is the automatic landing situation where the pilot's task is to monitor the

instruments for possible malfunctions. In the automatic approach, the command bars are inactive. In the manual approach, the pilot controls the aircraft by using the control information provided by the command bars.

Results of Computer Simulations

In all of the computer simulations, the ILS approach starts at an altitude of 460 meters, and a distance out of 10,770 meters. The aircraft automatically remains on course and on a glide slope of 2.5° , airspeed of 85 meters per second (165 knots) and a vertical speed of -3.7 meters per second.

Fixed Look Points.- Since the computer algorithms for look-point calculation is dependent on the user selected weights, initial runs were taken where the look points were read in and kept on each display for three or more time steps. In a typical run, the variances of the estimation of the state values from the initial observation are high. As each display is scanned, the estimation variances of the state variable(s) associated with that display converge rapidly to some limit. This limit is controlled by the inherent system variance (noise or turbulence) in the particular variable. The convergence time is controlled by the accuracy with which the variable information is displayed.

These convergence limits were used to get approximate values for the weights to be used in the calculation of look points in other runs. Figure 11 and Table 1 show typical data from this process. The values displayed here are the weighted standard deviations of the variables. The weights in this case were calculated so that all variances converged to approximately the same values. The variance of range (x) was the largest and was given a weight of one. The other variables were weighted such that their variances converged to the minimum variance of x, which was 45.9. For example, the weight

for σ_θ is 300. That is because the smallest value of σ_θ at time 22 was .154 minutes of arc.

Once these variances have converged to some value, they will either remain close to that value or start to increase. This depends on the acuity of the display associated with that variable with respect to the present look point. The size of the increase is associated with the system noise of that variable as compared to the present value of the variance of estimation.

In the example shown in Figure 11 and Table 1, the first look point is the airspeed display. Correspondingly, the weighted values associated with \dot{x}_r , 89.6, is much lower initially than other values, which are 909 up to 1,450. The \dot{x}_r value drops to 47 in three steps. As the look point goes to the other displays which do not contain pitch information, the pitch value climbs slowly to 78 (time step 13). The rate of this climb depends upon the location of the look point at any given time; for example, from time 4 to 7 the look point is on the VSI. This is the furthest instrument from the airspeed indicator. During this time period $\sigma_{\dot{x}}$ increases at a rate of about 2.1 per time step. Likewise, at times 16 to 22 the look point is on the eight ball which is the closest instrument to the airspeed indicator. During this time, $\sigma_{\dot{x}_r}$ increases at about 1.3 per time step. Similar responses can be seen with the eight ball $-\sigma_\theta$, VSI $-\sigma_{\dot{z}_r}$, and altimeter $-\sigma_{z_r}$. A somewhat different response is seen with the GSI $-\sigma_{z_r}$. This is because the GSI is related to both x_r and z_r . Thus, the GSI look point reduces both σ_{x_r} and σ_{z_r} . Also, when the altimeter look point is taken, σ_{x_r} continues to decrease. This is because of the high correlation between x_r and z_r when looking at the GSI. The altimeter look point reduces this correlation or confusion factor and thus reduces both σ_{z_r} and σ_{x_r} .

When using the look-point optimization, the look point is not read in, except initially; but it is determined as the

display which maximally reduces either the sum total weighted variances (weighted trace of the covariance matrix) or the predicted largest weighted variance. (Note: This prediction is based on keeping the present look point.)

Table 2 shows an example of the weighted mini-max process. This table shows the next look point is the center of the display associated with the variable having the highest weighted variance at the present state. The only exception being at times 11 and 22. This is because the next look-point criterion is based on the prediction variance for the present look point. The table shows the present estimation variance. At step 10, σ_{x_r} and $\sigma_{\dot{x}_r}$ have very close weighted values. The airspeed is chosen at step 11 because the σ_{x_r} prediction is larger. The same is true at step 21 where σ_{z_r} , $\sigma_{\dot{x}_r}$, and σ_{z_r} have similar values. Here σ_{z_r} predicted is larger than $\sigma_{\dot{x}_r}$ or σ_{z_r} .

Variance Weight and System Noise.- The above results show that the model behaves generally in a manner similar to human behavior and follows a pattern that is intuitively reasonable. The optimized look-point procedure is dependent on the selection of weights and the determination of the system variation (noise). Here, the weights are considered to be constant over time; the same for the system variation parameters. This assumption is probably valid for short periods of time but certainly not for different flight regimes (such as takeoff, landing, in flight, approach, etc.) or stages of the same regime (in-flight turn, descent, final approach, etc.). Also, the look point selected by the human reflects his opinion of how the system noise is effecting his variable estimation. His opinion of this noise is probably much larger than the actual effect. For example, if the controller does not look at the airspeed indicator for some period of time, the variation of \dot{x} estimation will grow, but his estimation of this growth is probably much larger than

reality. Thus, he feels he must glance at the airspeed indicator sooner than necessary to bring the \dot{x} variance down to a reasonable level.

A computer algorithm for determining the controller weights can be devised. But this algorithm must somewhere include some user determined parameters, such as allowable variance limits for each variable. Although this type of controller may logically be closer to the human thought process, it would still generate scan patterns dependent upon the input user parameters just as the present system is dependent on the input controller weights. The present configuration has the advantage of expediency and savings in computer time.

Results of Comparing Automatic and Manual Approach

With some of these ideas in mind, an attempt was made to run simulations comparing two real-life simulations. One is the automatic ILS approach where the pilot monitors the five previously discussed instruments (eight ball, glide slope indicator, altitude, vertical speed indicator, and airspeed indicator). The other is the manual ILS approach. The manual approach has the same instruments but also includes the horizontal and vertical command bars. In the real-life automatic situation, the pilot continually scans all five instruments. In the manual approach situation, the pilot tends to fixate on the command bars and occasionally glance at the other instruments.

Automatic Approach.- Table 3 and Figures 13 and 14 show the results of a six and one-half second simulation of the monitor situation. The time step is one eighth of a second. The system variation parameters are shown at the top of the table along with the weights used for the optimization routine. The weighted standard deviation values are shown in the table and plotted in the graph.

The graph of this data is shown in two parts. Figure 13 has the first second (8 time steps) during which the weighted values begin converging in large steps to the lower limits. Figure 14 shows the remaining time (starting at the sixth time step). Here, the values intertwine, each one growing to a point that requires a look point at the corresponding display. The system seems to converge all variables to values between 30 and 40. This occurs around the sixteenth time step or two seconds of scan time. The look points at each time step are shown at the top of the graph. The symbol on the look point graph indicates the variable being reduced in variance by that look point.

For example, in Figure 14 at time 5 the largest value is for range (x symbol on graph). Thus, at time 6 the look point (top of graph) is on the GSI. At time 6 the highest value is pitch (symbol = θ) so that the look point at time 7 is the eight ball. Correspondingly, the values associated with the present look point show a marked decrease over the present time step. For example, at time 8 the look point is the altimeter; from time 7 to 8 the altitude (symbol = Δ) drops from 56 to 33.

Figures 13 and 14 show only a portion of this run. The remaining time not shown demonstrates a similar pattern to times 16 through 26. Figure 15 shows the look points for the total 52 time steps.

The transition frequencies for the different displays are shown in Table 4. Figure 16 shows the transition probabilities in a more graphic form. Note here that the glide slope has the highest look-point frequency. The glide slope was looked at 15 time steps out of 52. The eight ball was next at 14, followed closely by the altimeter at 11. The reason for this can be seen in the table and graph of the weighted values. When not looking at the displays associated with pitch, range, or altitude, the weighted values grow at two to three units per

time step. This can be compared to the airspeed and altitude rate values which grow at 1 to 1.5 units per step.

Manual Approach.- In this situation, the command bars were added to the display. The problem here is to select values for the pilot's perceived command bar system variances and the weights for look-point determination that reflect reality. If the variances and weights are too high, the predicted command bar weighted variance values jump to a level above the other variances even with continued fixation on that look point; this causes the look-point controller to ignore the other display for long periods of time. If these values are too low, then the command bars will be ignored or only glanced at occasionally. Several runs were made with different weights and system variances. The results of the fixed run is shown in Tables 5 and 6 and Figures 17, 18, and 19. Table 5 shows the various parameters used, the look points for 25 time steps, and the weighted standard deviation values. Here, the location of the vertical and horizontal command bars and the eight ball is the same. The separation of their look points was determined by the variable whose weighted variance was being minimized. For example, at time 3, the pitch value is 187 so that the eight-ball look point is selected for step 4. (This reduces not only the pitch values but also the values associated with the command bars (120 to 21).) But at time 6 the cb_h has a larger predicted value indicating the look point at 7 was taken in order to decrease the cb_h value. The command bars have values very close to one another throughout the total run. The slight differences are due to random movement generated by the simulation. This locates the command bars slightly off the center of the eight-ball display thus slightly affecting the acuity of the command bars.

The transition frequencies (Tables 6A and 6B) are shown with the

command bars and eight ball separated and also with their combined frequency. Figure 20 shows the probabilities combined. The graphs of these data and the look points show how the values of all variables grow relatively slowly compared to the command bars' values. Because of this, the look point is always going to the command bars then going to various other displays from there.

AREAS OF FURTHER INVESTIGATION

The preliminary results from this program indicate much promise as a model of the human visual scanning process, but many questions remain unanswered. To be of use in evaluating displays for possible human use, the program must be able to imitate human behavior on present displays at some level of realism.

Time Step.- The time step for the Kalman filter does not necessarily have to be constant. The filter processes information after every time step. Is it possible that the human operator processes visual information at different rates? It is possible that little or no processing occurs when the instrument is first perceived, but then the information process rate could increase the longer the display is observed. In other words, how long does one fixation take? If a fixation is repeated (keeps the same look point), is the time step the same, or does it take less time to get information once the look point is established?

Variance Weights.- In the look-point selection algorithm, much emphasis is placed on the weights for the variables' variances. Are these weights really constant? Specifically, even during the same flight pattern do the weights change, say increasing the longer the pilot does not look at the displays associated with the variables?

System Noise (Variance).- The relative size of the system noise of the state variables and the relative weights are also important in the scanning process. In setting the system variation of the state variables, should realistic values be used or should they be values that reflect how the pilot perceives them?

Display Modification.- The importance of comparing these various options of time step, system noise, and weights becomes obvious when comparing two or more display types with the same state variables. If the human pilot does have fixed weights and fixed system noise for the various variables, then these values should not change even under radically different displays. These weights are for the state variables, not for the displays. Any change of scan and accuracy of estimation should be due to the displays.

One topic only mentioned in passing was the complexity of various look points or displays. One measure of this is the absolute size of the correlations between the state variables. Should this complexity be used not only as a secondary measure to compare display setups but also be used for finding optimum look points?

Closed-Loop Controller.- In the present program the aircraft dynamics including the closed-loop control system are not simulated. A perfect controller is assumed; that is, the aircraft's state variables (no matter how large the variances in their estimation) are at each time step perturbed about their nominal value by some random variable with a fixed probability distribution.

This is certainly in contrast to reality with manual control. Here, as the pilot's errors in the estimation of the state variables becomes larger, the deviations from the nominal flight path will increase. It would appear to be worthwhile to gain more insight into how much error in

the state variable estimation a pilot can afford to make his landing acceptable.

REFERENCES

1. Burgin, George H. and Mout, Michael L. "A Computer Program for the Use of Sensitivity Analysis in Display Evaluation," NASA CR-145060, Contract No. NAS1-13734, Decision Science, Inc., San Diego, California, April, 1976.
2. Kalman, R. E. A New Approach to Linear Filtering and Prediction Problems. J. Basic Eng. 82 (1960).
3. Kalman, R. E. New Results in Linear Filtering and Prediction Theory. J. Basic Eng. 83 (1961).
4. Sorenson, H. W. Kalman Filtering Techniques, Advances in Control Systems. Vol. 3, C. T. Leondes, Ed., New York: Academic Press, 1966.

Appendix A

Derivation of Simplified Forms of the Gain Matrix

This appendix show the derivation of simplified forms of the gain matrix and covariance matrix from the Kalman Filter process. These forms are for both the present time step and the prediction.

We first derive the following lemma.

Lemma: Let B and R be positive definite symmetric matrices and let H be any matrix (including rectangular). Let A be defined by

$$A = B - BH' [HBH' + R]^{-1} HB.$$

Then

$$A^{-1} = B^{-1} + H'R^{-1}H.$$

Proof: Assume the above form for A^{-1} , then

$$\begin{aligned} AA^{-1} &= [B - BH' (HBH' + R)^{-1} HB] [B^{-1} + H'R^{-1}H] \\ &= I - BH' (HBH' + R)^{-1} H + BH' R^{-1} H - BH' (HBH' + R)^{-1} HBH' R^{-1} H \\ &= I - BH' [(HBH' + R)^{-1} H - R^{-1} H + (HBH' + R)^{-1} HBH' R^{-1} H] \\ &= I - BH' [(HBH' + R)^{-1} - R^{-1} + (HBH' + R)^{-1} HBH' R^{-1}] H \\ &= I - BH' [(HBH' + R)^{-1} (I + HBH' R^{-1}) - R^{-1}] H \\ &= I - BH' [(R + HBH')^{-1} (R + HBH' R^{-1} R) - R^{-1}] H \\ &= I - BH' [(R + HBH')^{-1} (R + HBH') R^{-1} - R^{-1}] H \\ &= I - BH' [I R^{-1} - R^{-1}] H \\ &= I. \end{aligned}$$

Now in the original Kalman Filter process

$$K_i = \Sigma_i |_{i-1} T_i' [T_i \Sigma_i |_{i-1} T_i' + \Xi_i]^{-1}$$

and

$$\begin{aligned} \Sigma_i |_{i-1} &= [I - K_i T_i] \Sigma_i |_{i-1} \\ &= \Sigma_i |_{i-1} - \Sigma_i |_{i-1} T_i' [T_i \Sigma_i |_{i-1} T_i' + \Xi_i]^{-1} \Sigma_i |_{i-1}. \end{aligned}$$

Now, since $\Sigma_i |_{i-1}$ and Ξ_i are symmetric positive definite we can

apply the lemma. This gives

$$\Sigma_{i|i}^{-1} = \Sigma_{i|i-1}^{-1} + T_{i|\Sigma_{i|i-1}}^{-1} T_{i|\Sigma_{i|i-1}}.$$

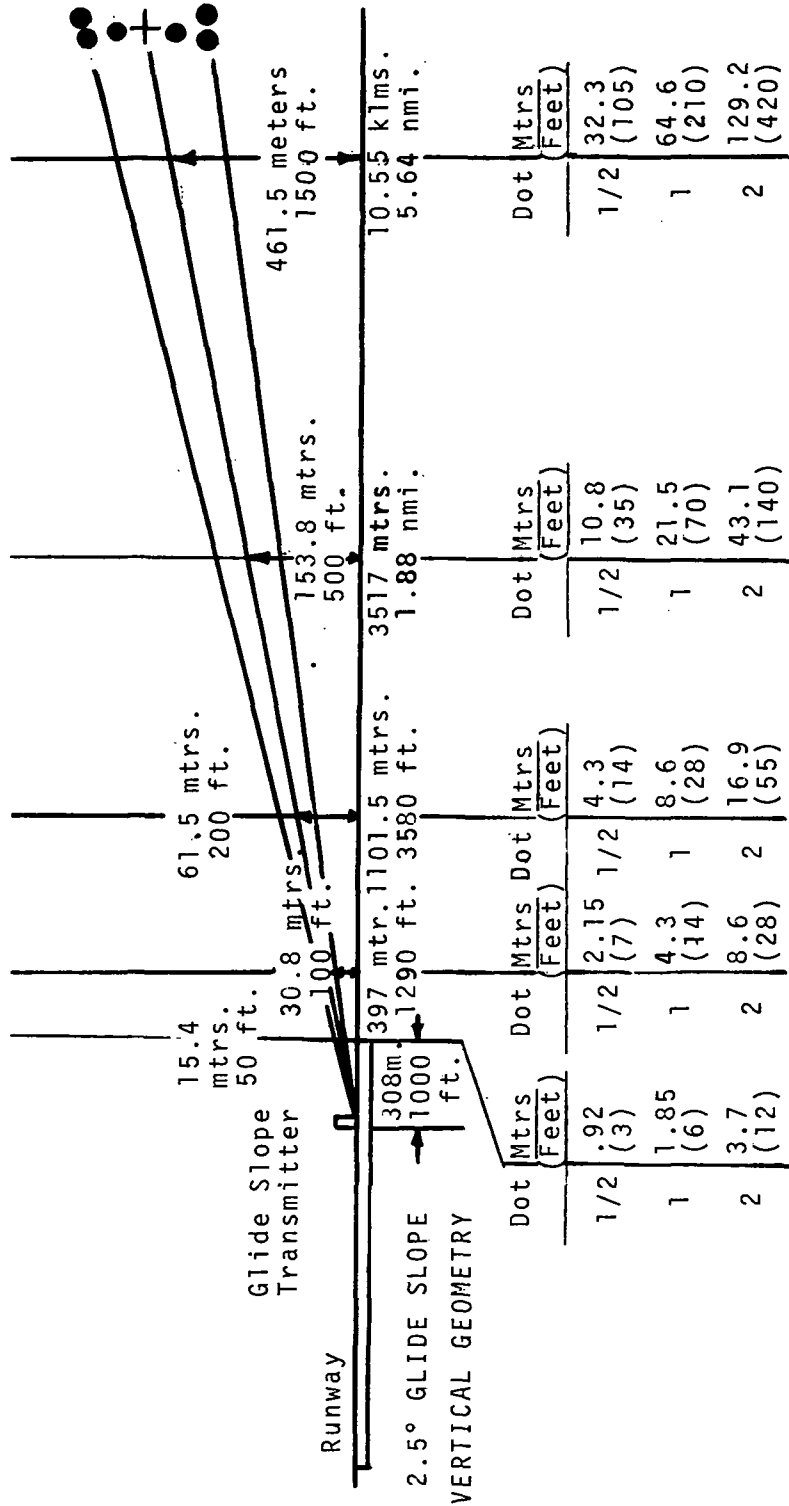
We can now write

$$\begin{aligned} K_i &= [\Sigma_{i|i}^{-1} \Sigma_{i|i-1}^{-1}] \Sigma_{i|i-1}^{-1} T_{i|\Sigma_{i|i-1}}^{-1} [T_{i|\Sigma_{i|i-1}}^{-1} T_{i|\Sigma_{i|i-1}}^{-1} + I]^{-1} \\ &= [\Sigma_{i|i}^{-1} (\Sigma_{i|i-1}^{-1} + T_{i|\Sigma_{i|i-1}}^{-1} T_{i|\Sigma_{i|i-1}})] \Sigma_{i|i-1}^{-1} T_{i|\Sigma_{i|i-1}}^{-1} \\ &\quad [T_{i|\Sigma_{i|i-1}}^{-1} T_{i|\Sigma_{i|i-1}}^{-1} + I]^{-1} \\ &= \Sigma_{i|i}^{-1} [T_{i|\Sigma_{i|i-1}}^{-1} (T_{i|\Sigma_{i|i-1}}^{-1} T_{i|\Sigma_{i|i-1}}^{-1} + I)^{-1} + \\ &\quad T_{i|\Sigma_{i|i-1}}^{-1} T_{i|\Sigma_{i|i-1}}^{-1} (T_{i|\Sigma_{i|i-1}}^{-1} T_{i|\Sigma_{i|i-1}}^{-1} + I)^{-1}] \\ &= \Sigma_{i|i}^{-1} T_{i|\Sigma_{i|i-1}}^{-1} [(T_{i|\Sigma_{i|i-1}}^{-1} T_{i|\Sigma_{i|i-1}}^{-1} + I) + \\ &\quad T_{i|\Sigma_{i|i-1}}^{-1} T_{i|\Sigma_{i|i-1}}^{-1} (T_{i|\Sigma_{i|i-1}}^{-1} T_{i|\Sigma_{i|i-1}}^{-1} + I)] \\ &= \Sigma_{i|i}^{-1} T_{i|\Sigma_{i|i-1}}^{-1} [(I + T_{i|\Sigma_{i|i-1}}^{-1} T_{i|\Sigma_{i|i-1}}^{-1}) (T_{i|\Sigma_{i|i-1}}^{-1} T_{i|\Sigma_{i|i-1}}^{-1} \\ &\quad + I)^{-1}] \\ &= \Sigma_{i|i}^{-1} T_{i|\Sigma_{i|i-1}}^{-1}. \end{aligned}$$

APPENDIX B

GLIDE SLOPE INDICATOR (GSI) RESPONSE

The chart below shows the response of the GSI to altitude durations above or below the glide slope at various distances from the end of the runway.



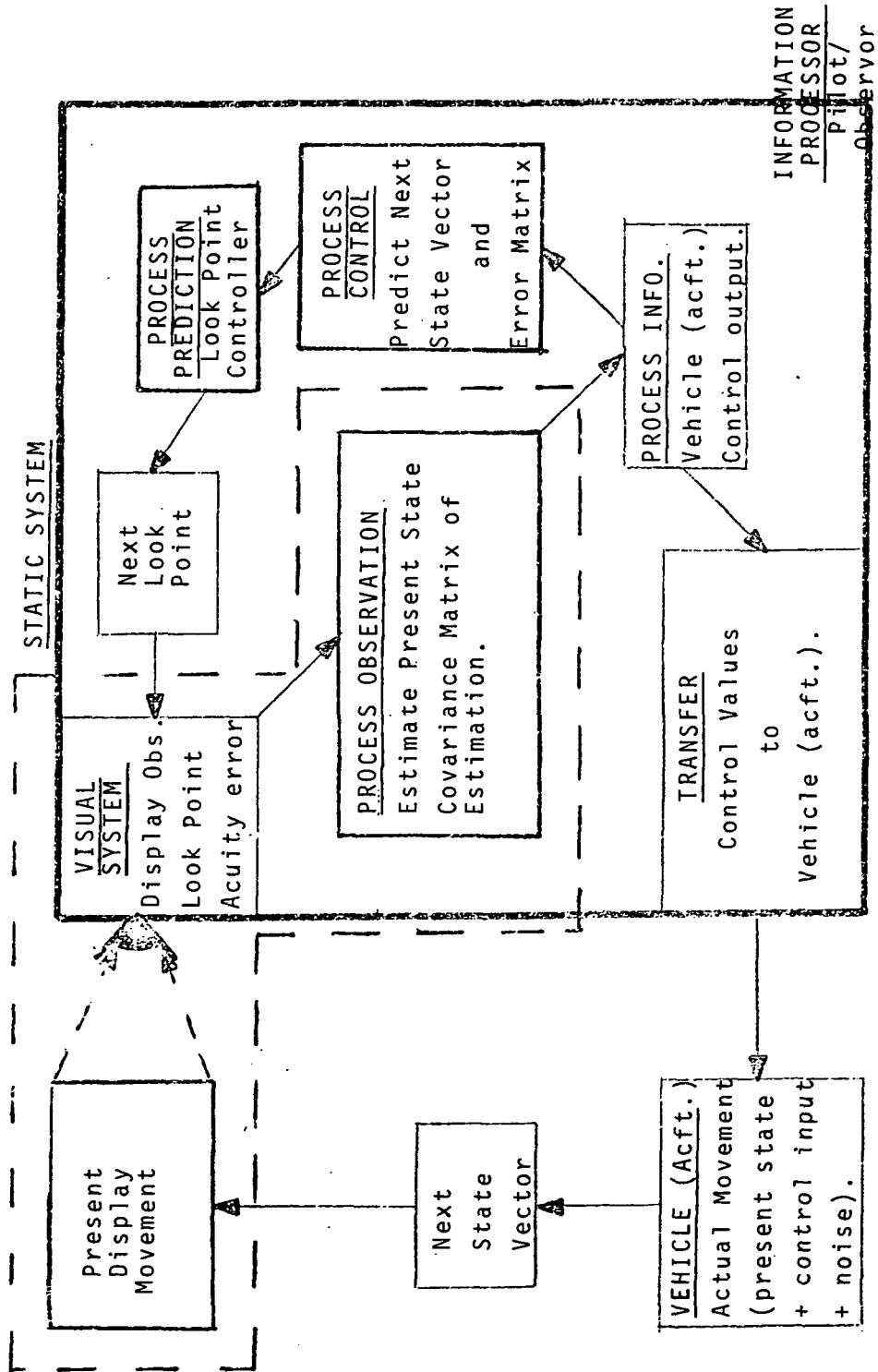
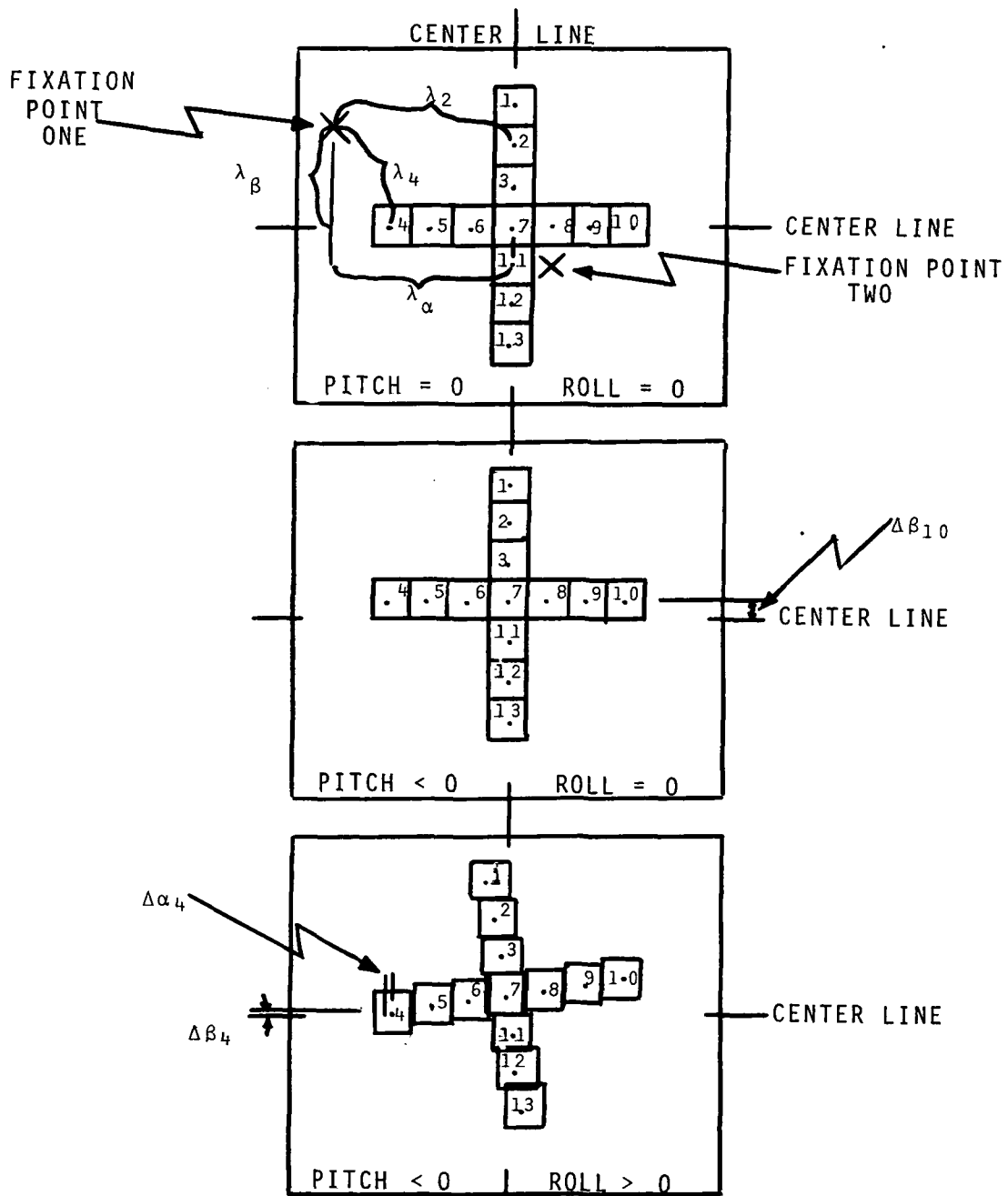
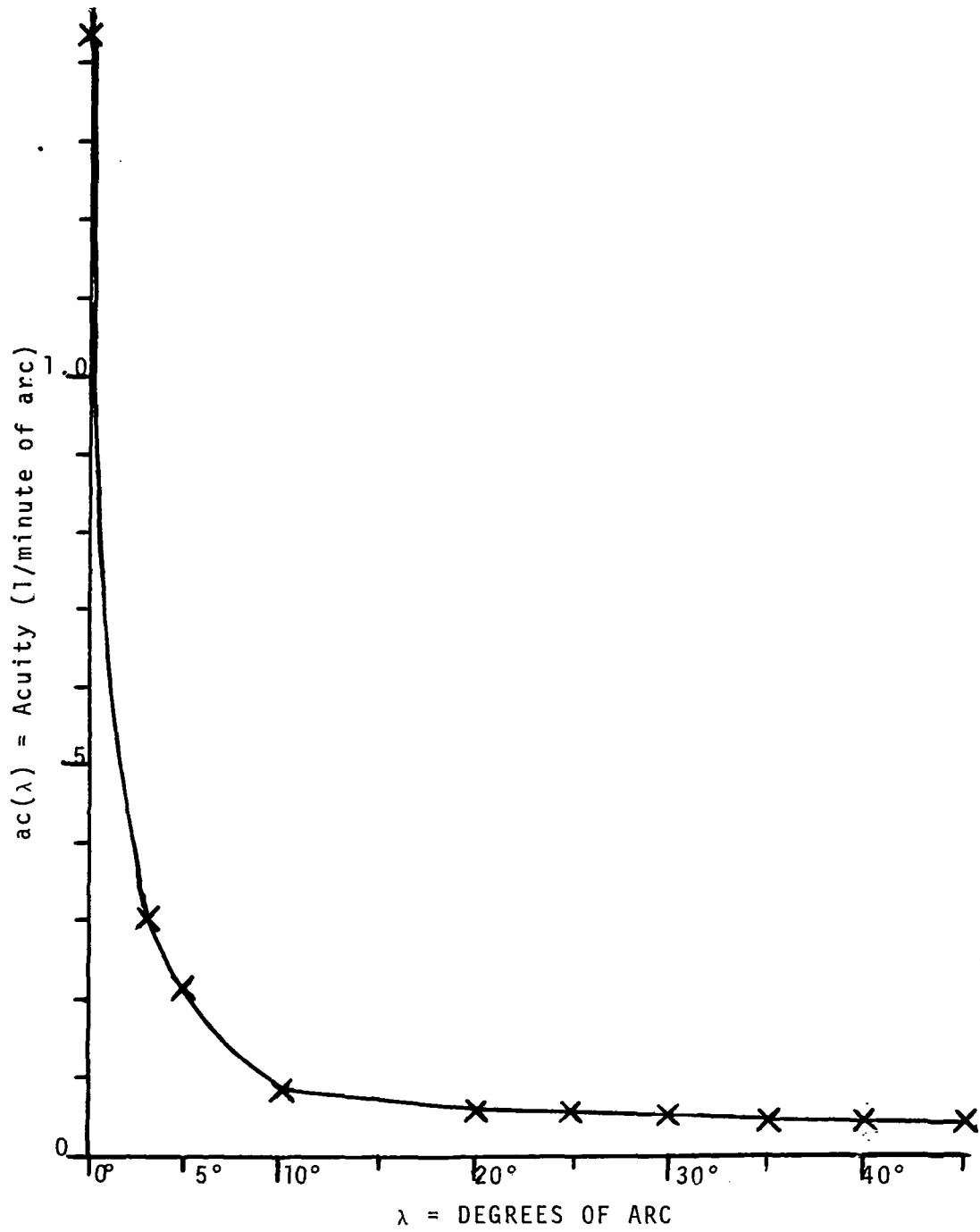


Figure 1
 Information Flow for Dynamic System
 (Dotted Lines - Static System)

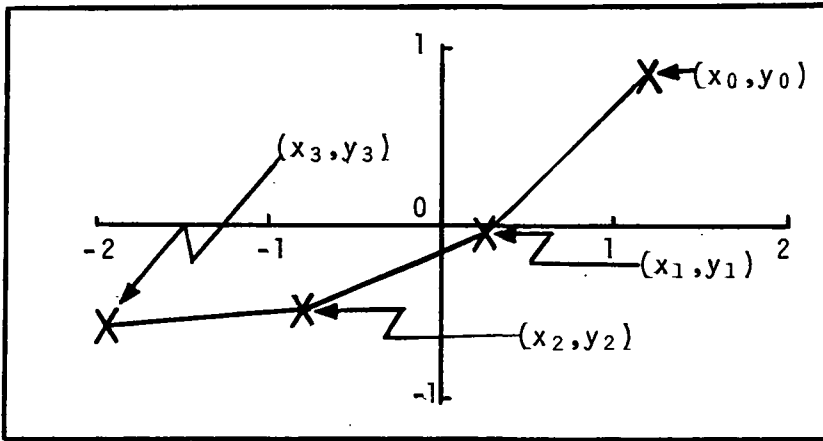


EXAMPLE OF A SEGMENTED ARTIFICIAL HORIZON DISPLAY MOVING IN THREE TIME STEPS

FIGURE 2



SAMPLE ACUITY FUNCION
 FIGURE 3 .



Time Step	x_i	$u_{x_{i-1}}$	$\gamma_{x_{i-1}}$	y_i	$u_{y_{i-1}}$	$\gamma_{y_{i-1}}$
0	1.2		.2	.85		-.15
1	.25	-1.0	.05	-.05	-1.0	.10
2	-.81	-1.0	-.06	-1.01	-1.0	.04
3	-1.91	-1.0	-.1	-1.09	0	-.08

$$x_{i+1} = x_i + u_{x_i} + \gamma_{x_i} \quad y_{i+1} = y_i + u_{y_i} + \gamma_{y_i}$$

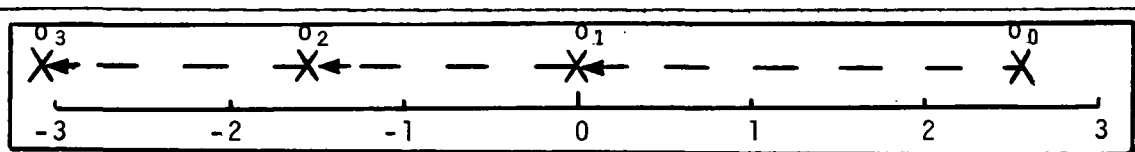
$$\underline{x}_{i+1} = A_i \underline{x}_i + B_i \underline{u}_i + D_i \underline{y}_i$$

$$\underline{x}_i = \begin{pmatrix} x_i \\ y_i \end{pmatrix}, \quad \underline{u}_i = \begin{bmatrix} u_{x_i} \\ u_{y_i} \end{bmatrix}, \quad \underline{y}_i = \begin{bmatrix} \gamma_{x_i} \\ \gamma_{y_i} \end{bmatrix}, \quad \text{cov}(\underline{y}_i) = \Gamma = \begin{bmatrix} .015 & 0 \\ 0 & .015 \end{bmatrix}$$

$$E(\underline{x}_0) = \begin{pmatrix} 1 \\ 1 \end{pmatrix}, \quad \Sigma_0 = A_i = B_i = D_i = I = \begin{pmatrix} 1 & 0 \\ 0 & 1 \end{pmatrix}$$

KALMAN FILTER PROCESS EXAMPLE — STATE EQUATIONS

FIGURE 4A



$$o_i = T_i x_i + \xi_i$$

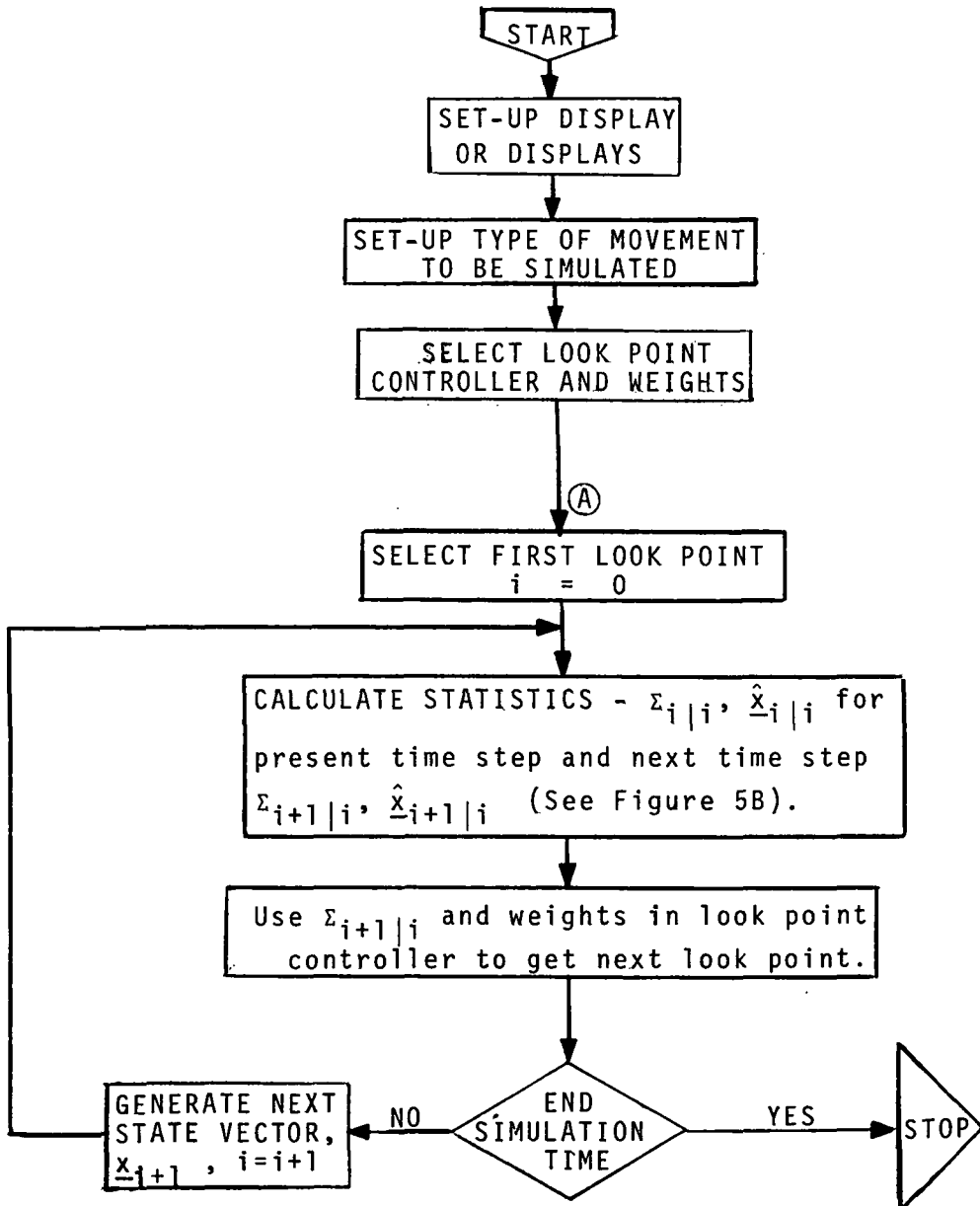
$$o_i = x_i + y_i + \xi_i$$

$$T_i = (1.1), \quad \text{cov}(\xi_i) = \Xi_i = 0.4$$

Time Step	o_i	ξ_i
0	2.55	.5
1	-.05	-.25
2	-1.57	.25
3	-3.1	-.1

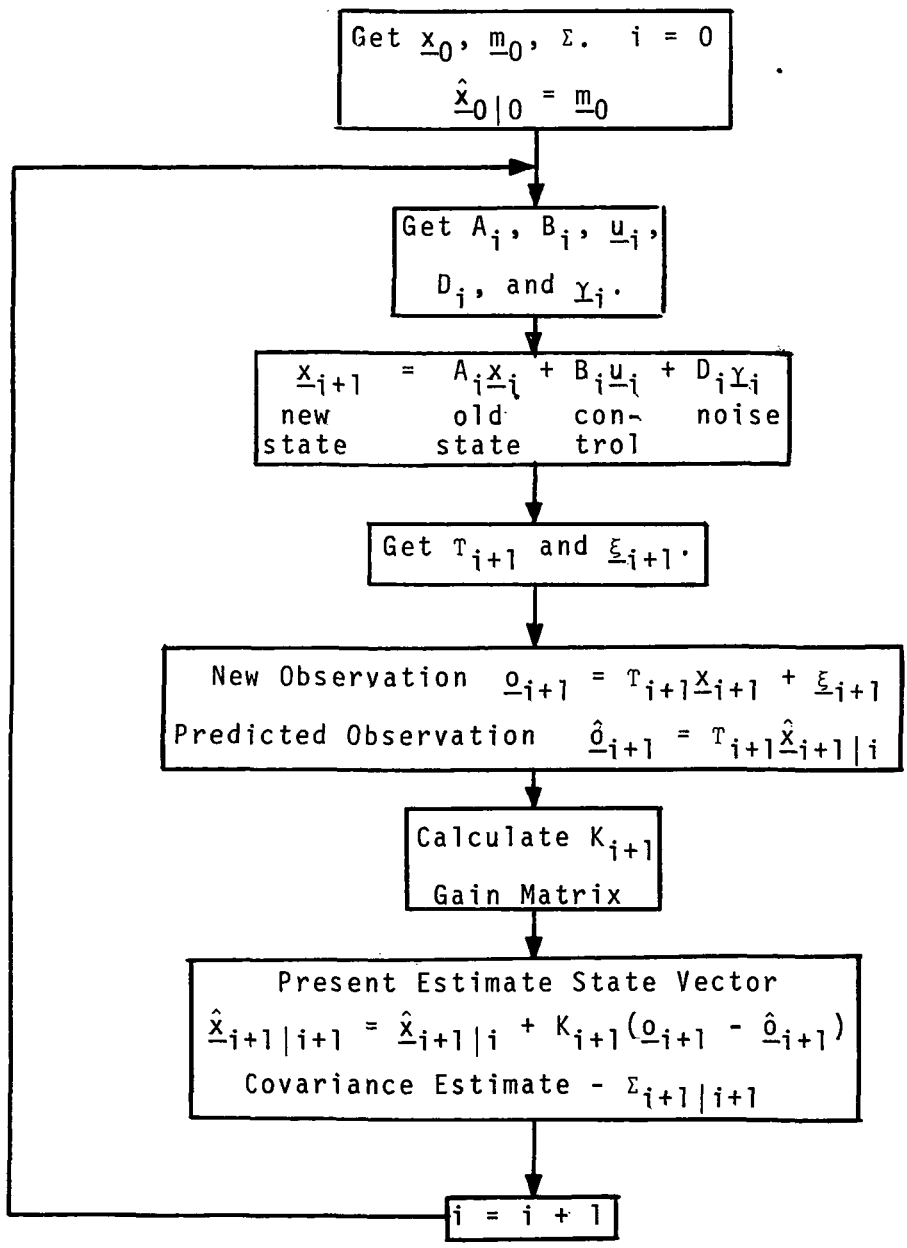
KALMAN FILTER PROCESS EXAMPLE — OBSERVATION EQUATIONS

FIGURE 4B



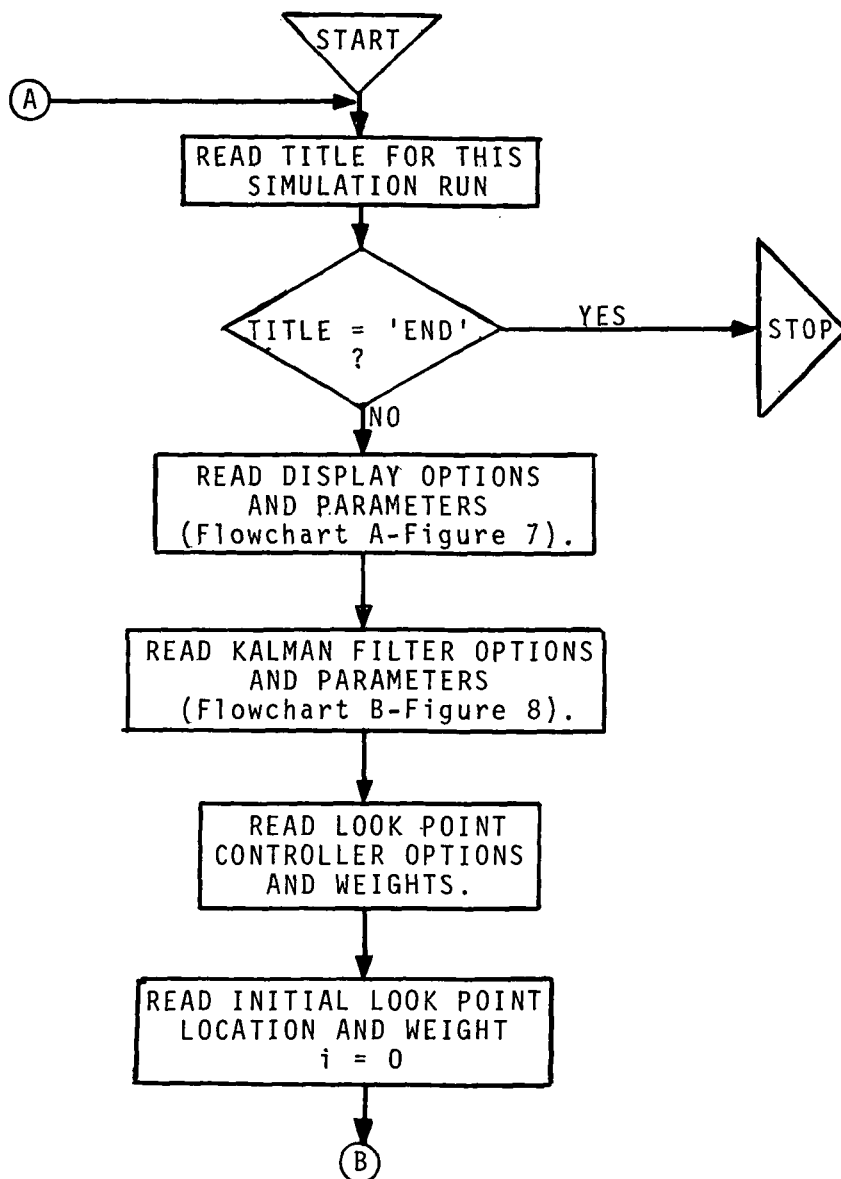
GENERAL MODEL FLOWCHART

FIGURE 5A



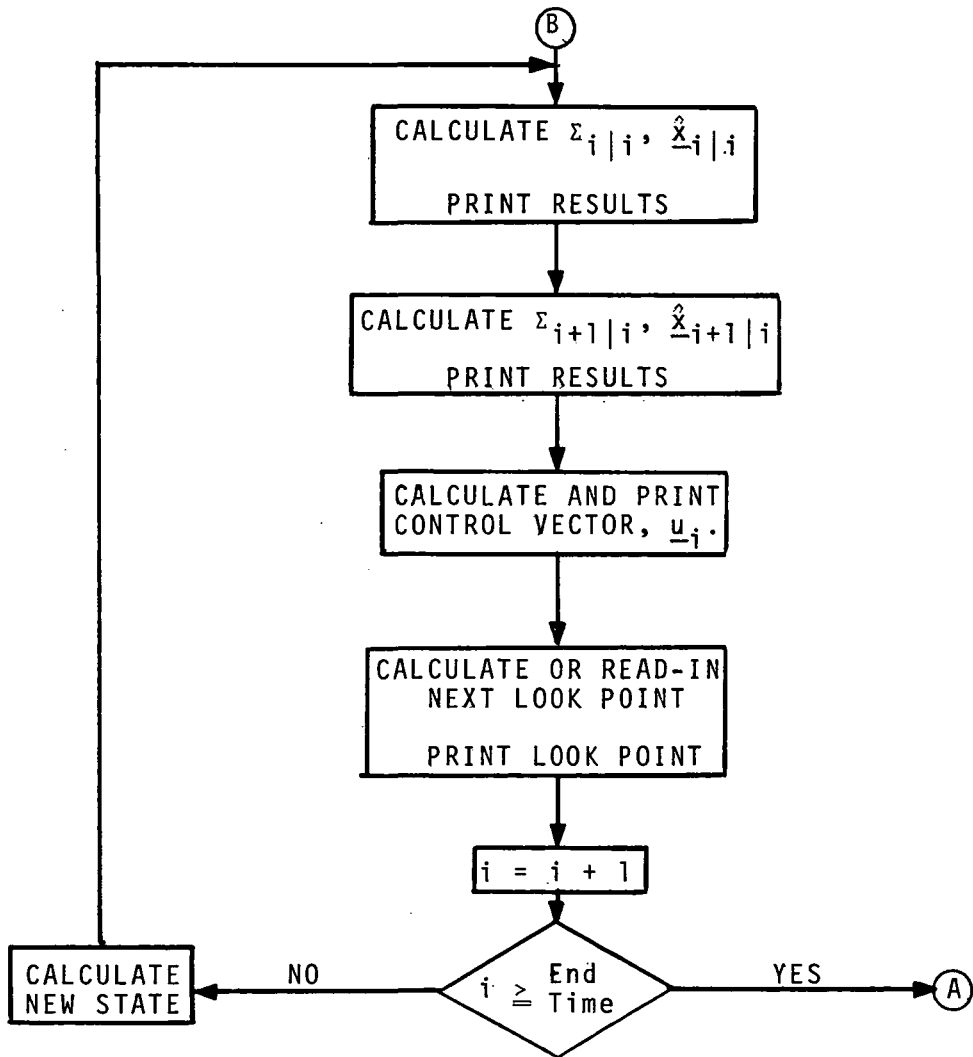
DETAIL FLOWCHART - KALMAN FILTER

FIGURE 5B



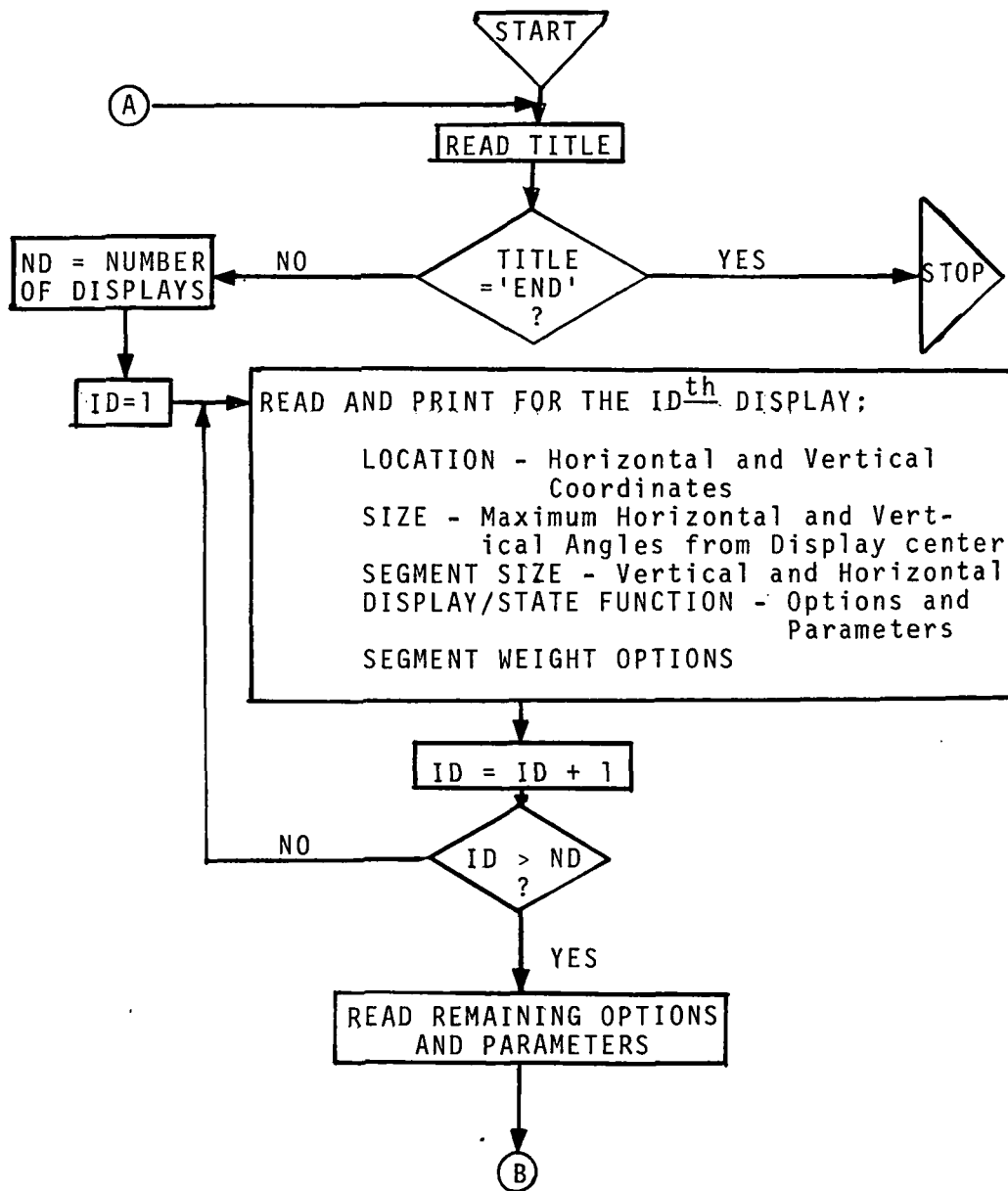
GENERAL COMPUTER PROGRAM FLOW CHART

FIGURE 6



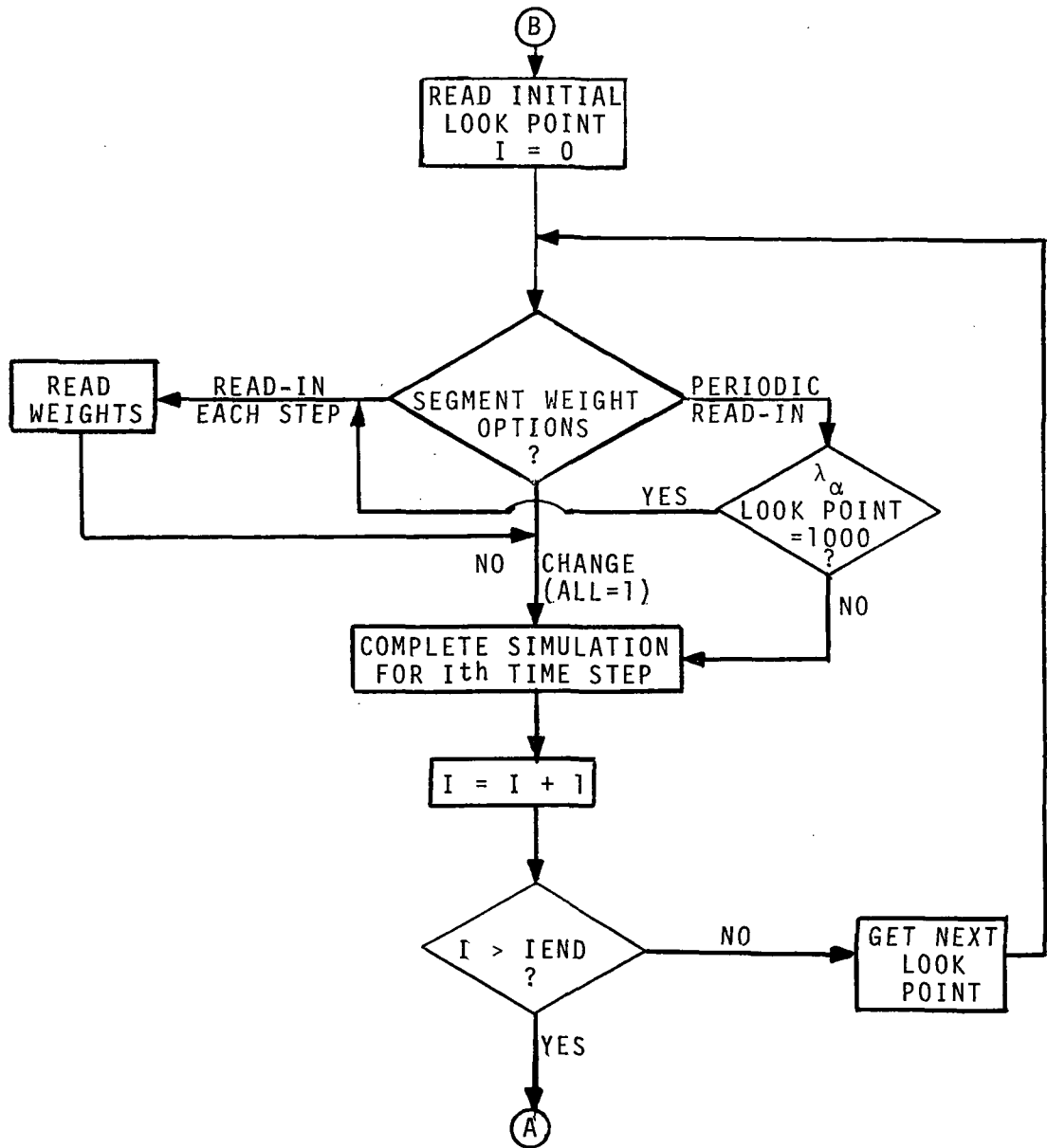
COMPUTER PROGRAM (Continued)

FIGURE 6 (Continued)



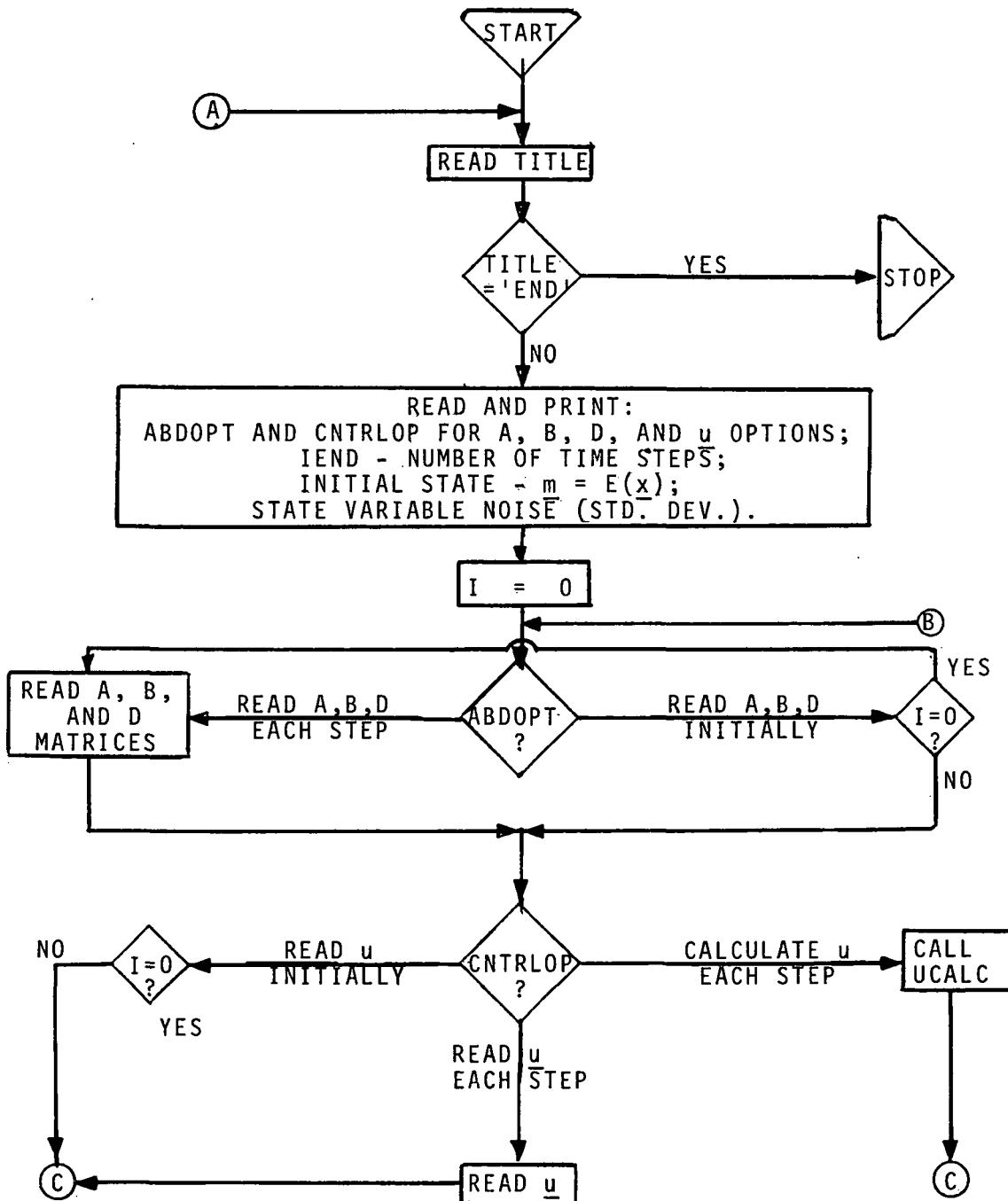
FLOW CHART A
DISPLAY OPTIONS AND PARAMETERS

FIGURE 7

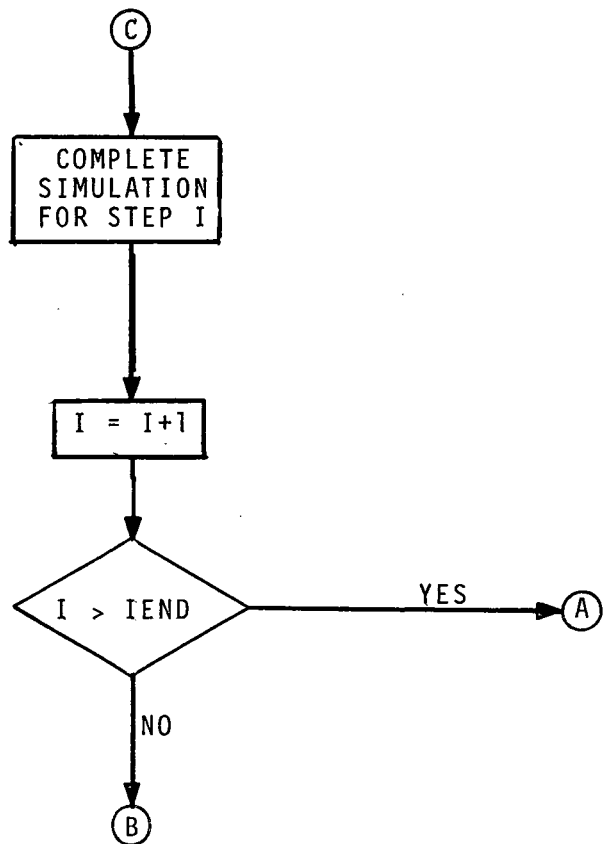


FLOW CHART A (Continued)

FIGURE 7 (Continued)

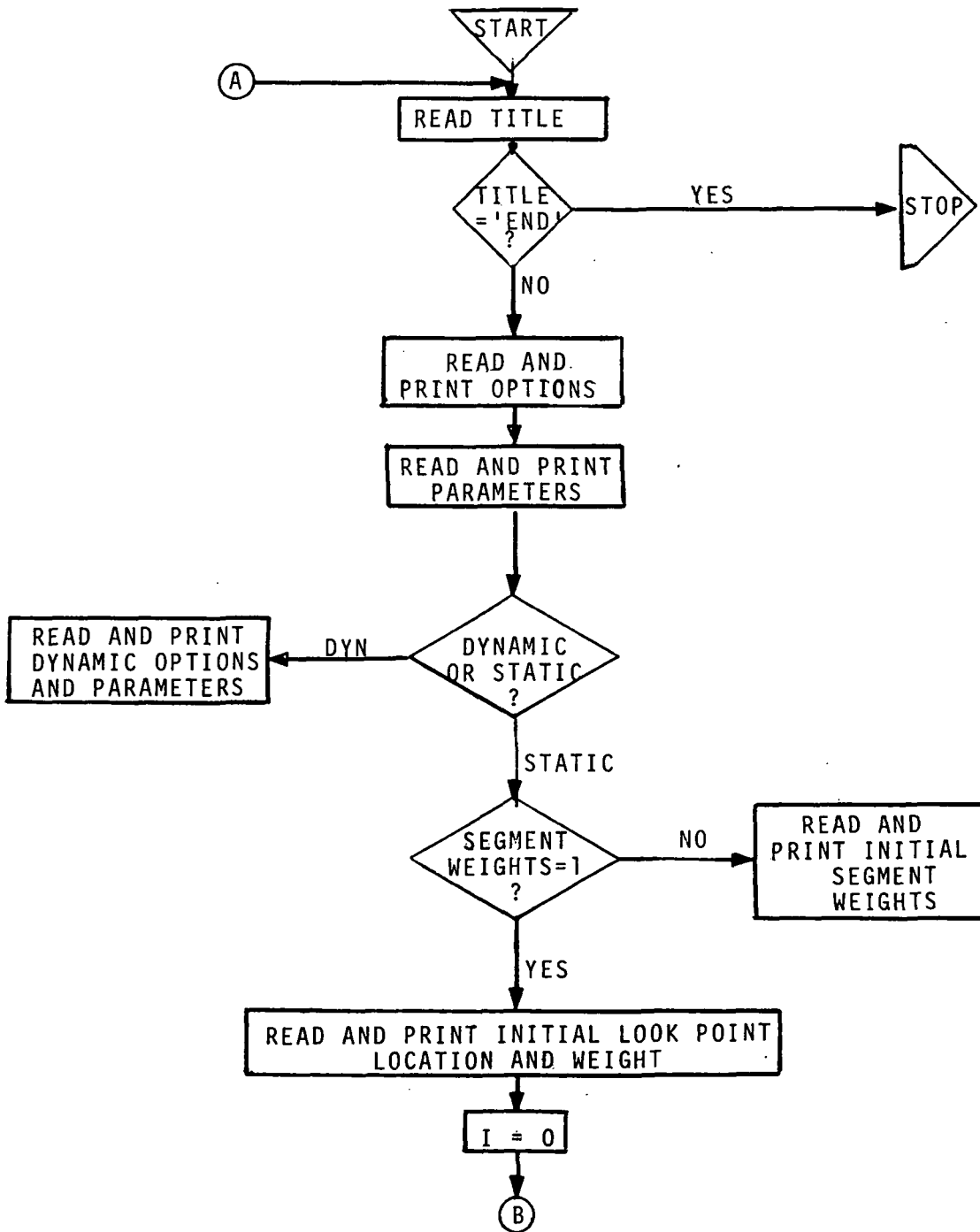


FLOW CHART B
KALMAN FILTER OPTIONS AND PARAMETERS
FIGURE 8



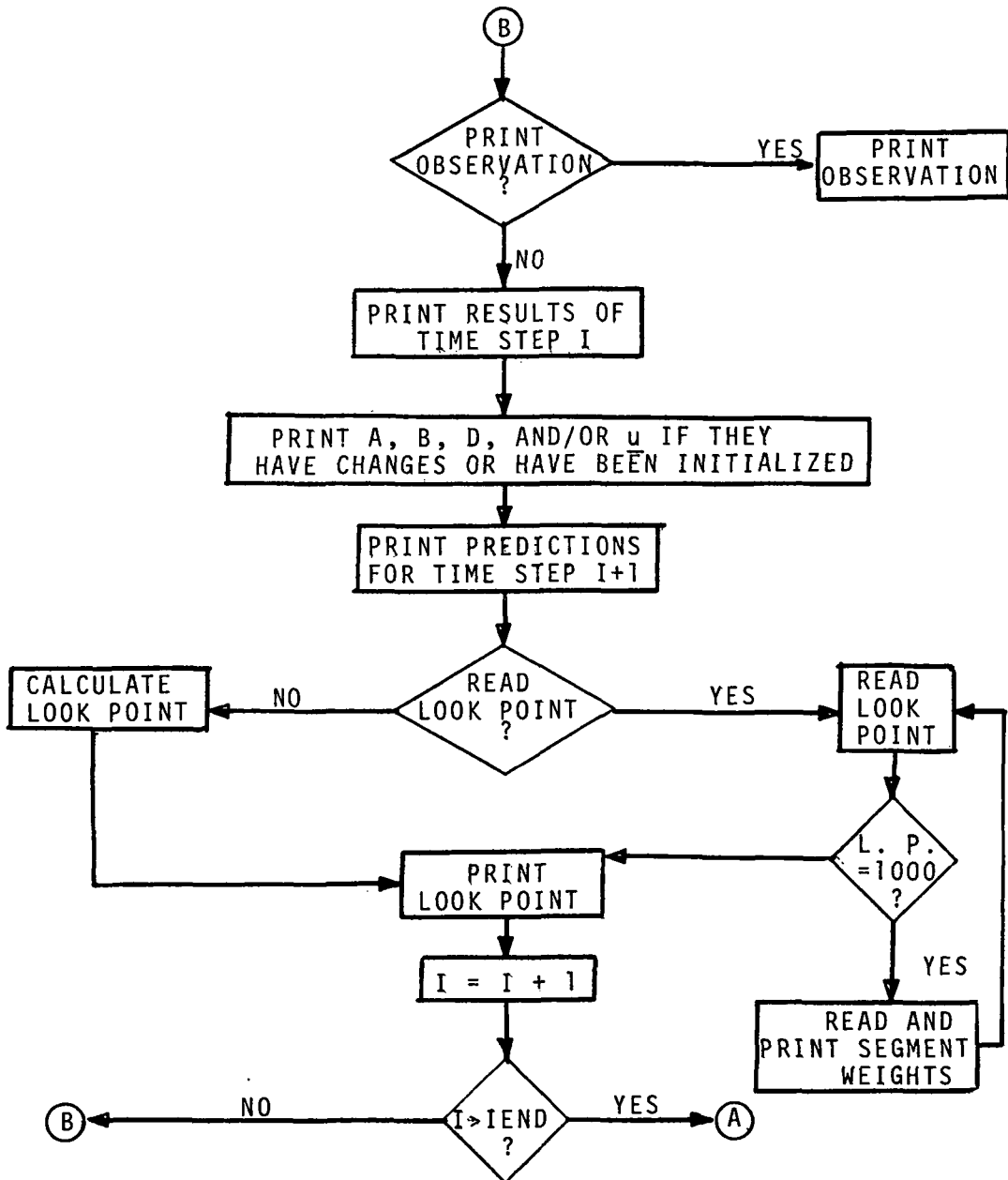
FLOW CHART B (Continued)

FIGURE 8 (Continued)



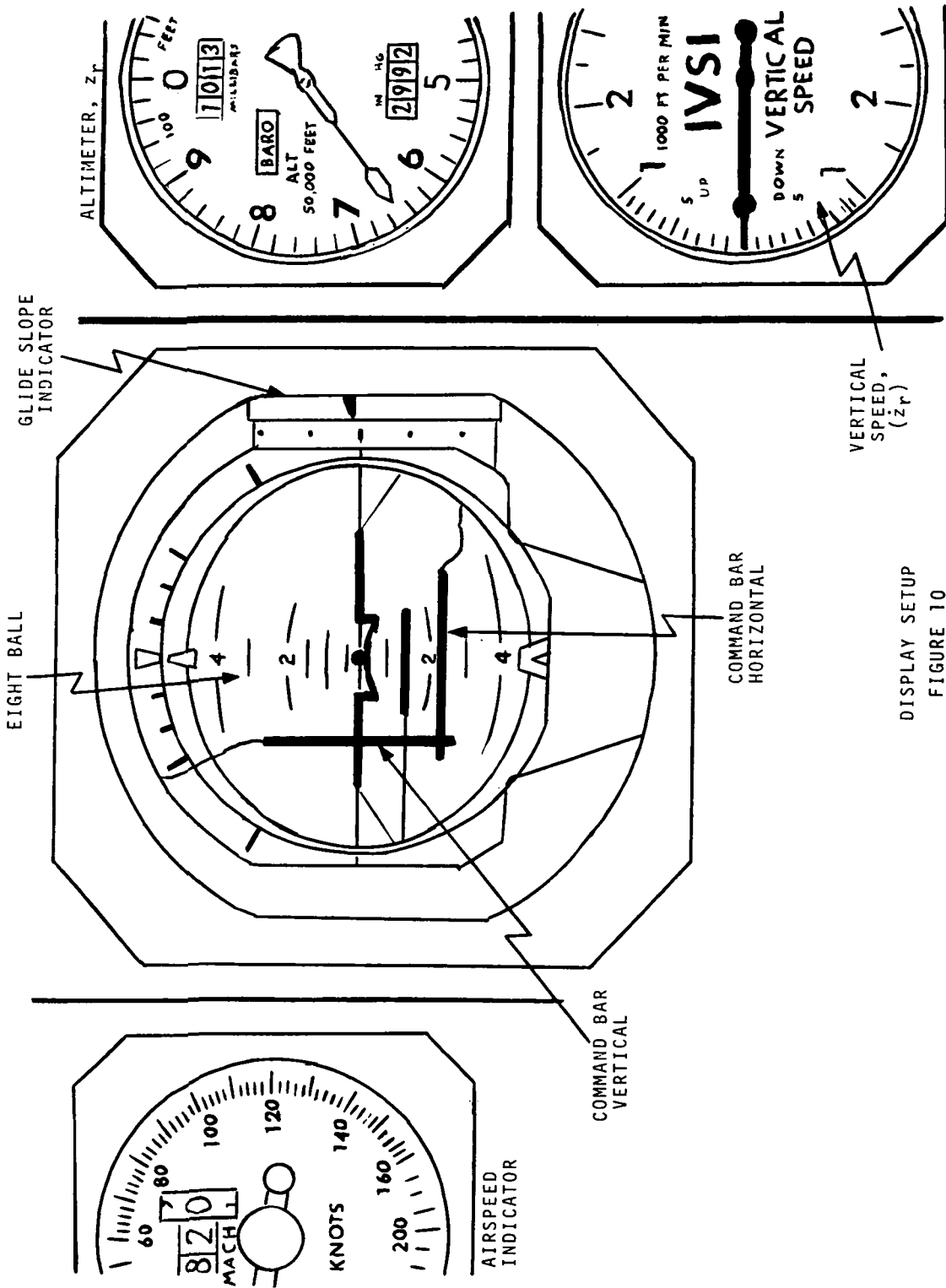
PRINT OPTIONS AND OUTPUT

FIGURE 9



PRINT OPTIONS AND OUTPUT (Conitnued)

FIGURE 9 (Continued)



DISPLAY SETUP
FIGURE 10

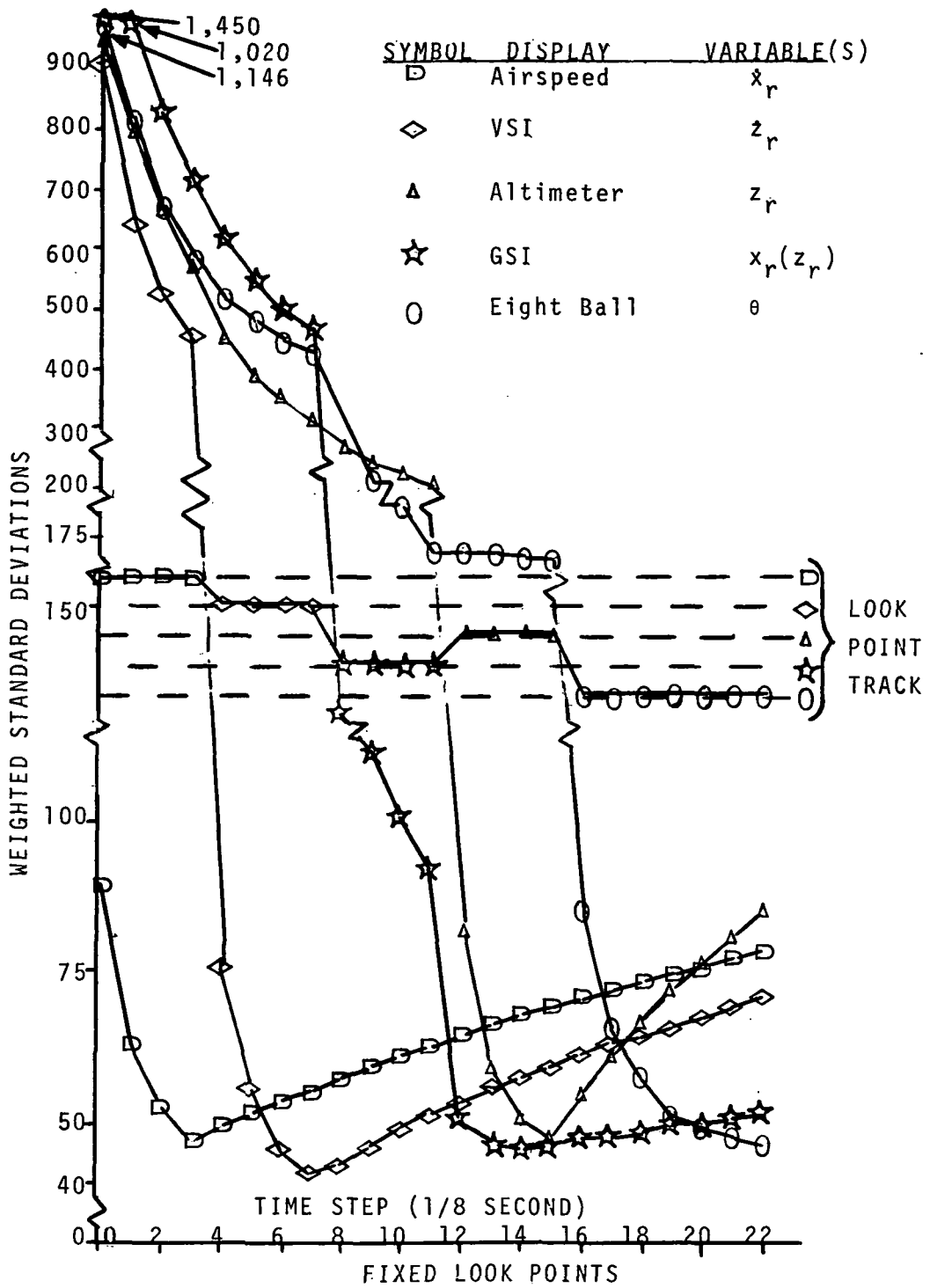


FIGURE 11

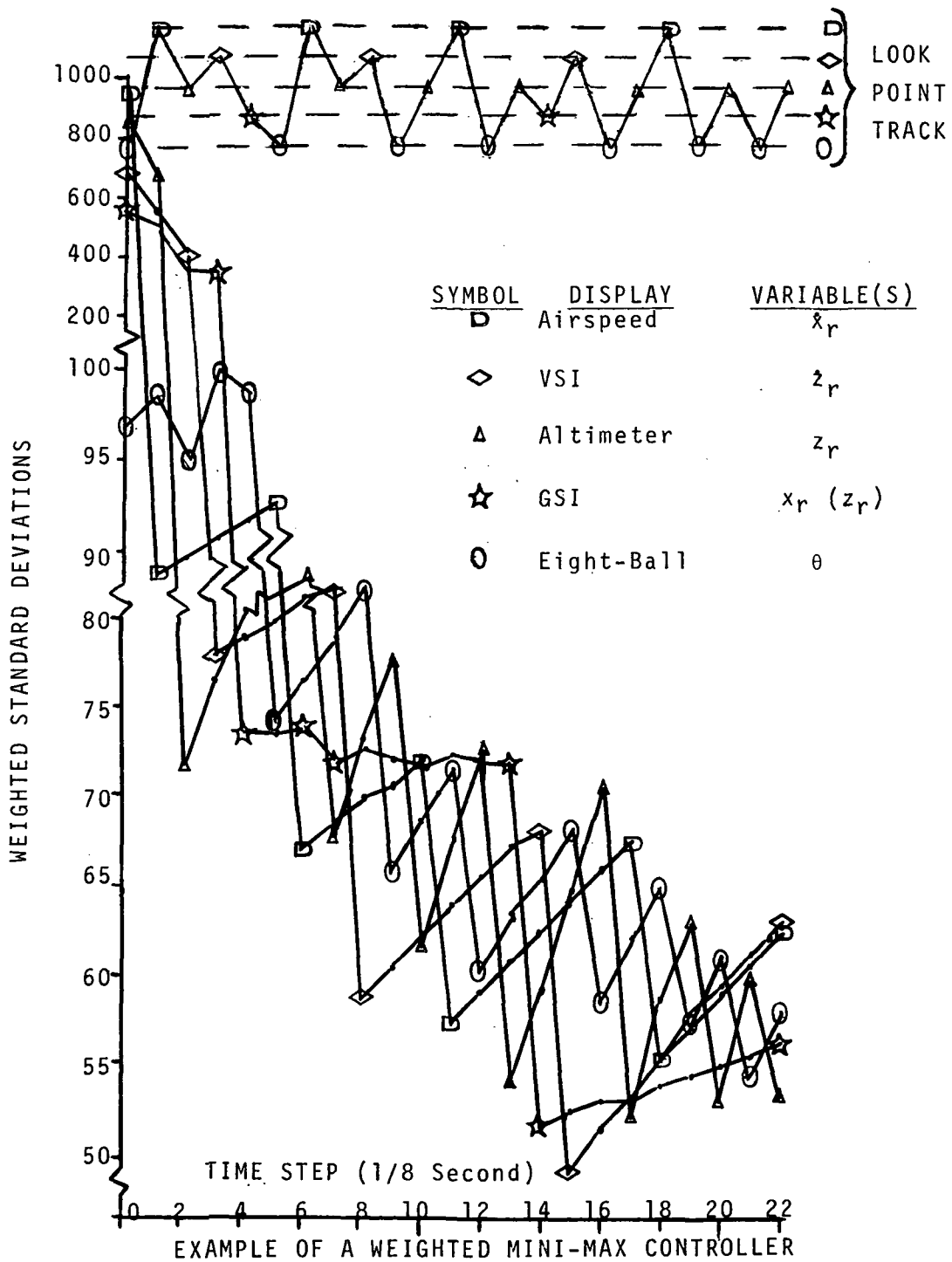
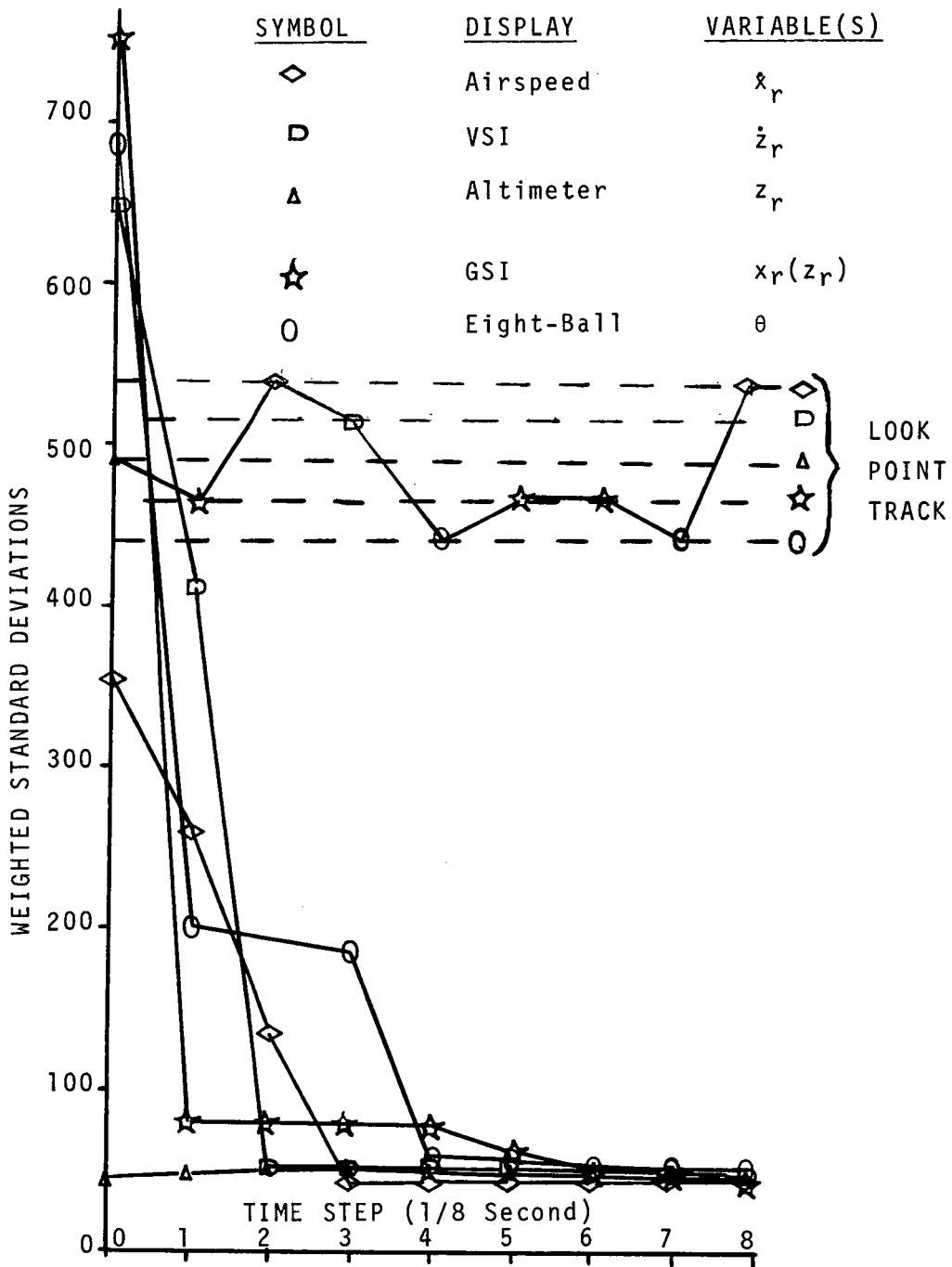
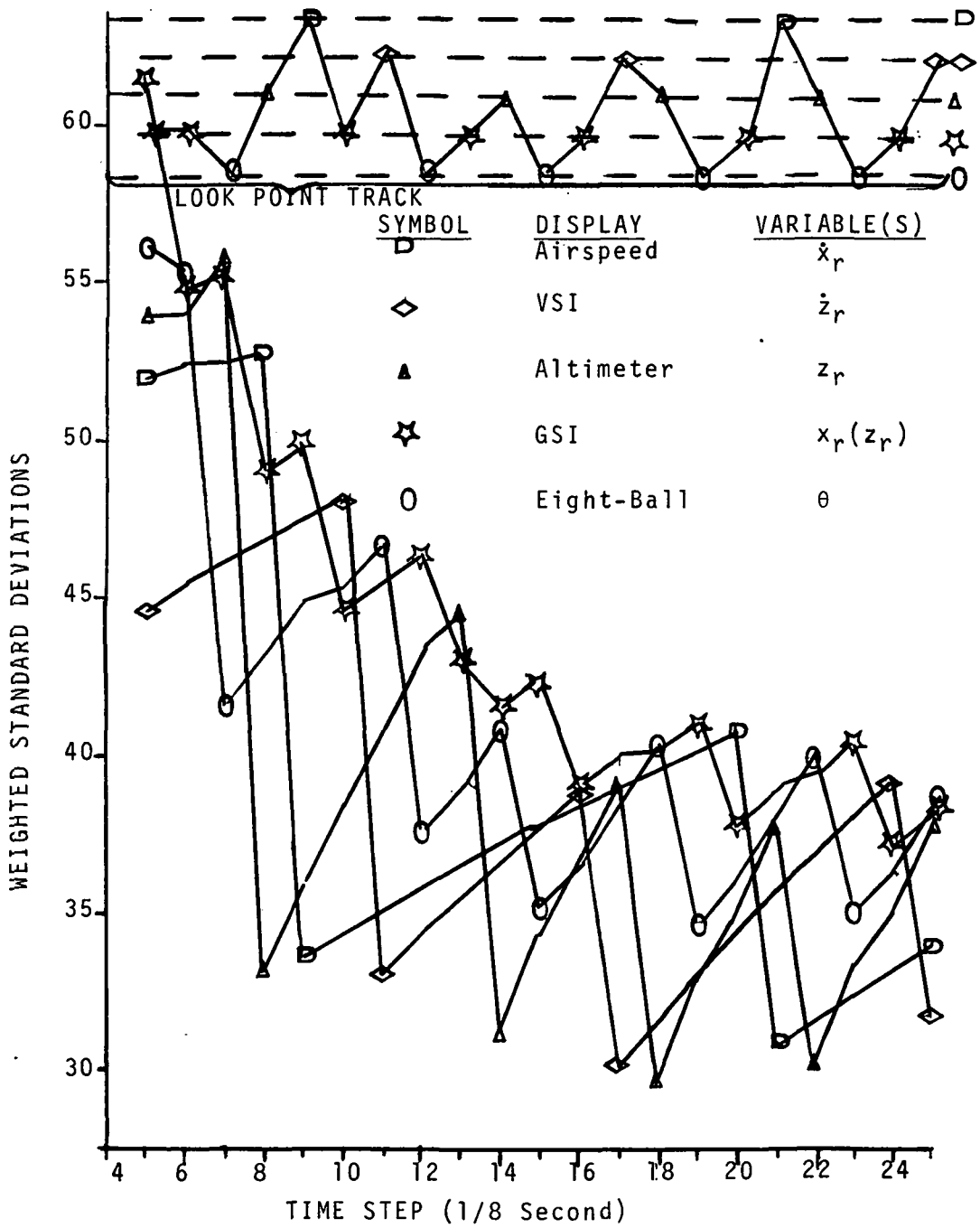


FIGURE 12



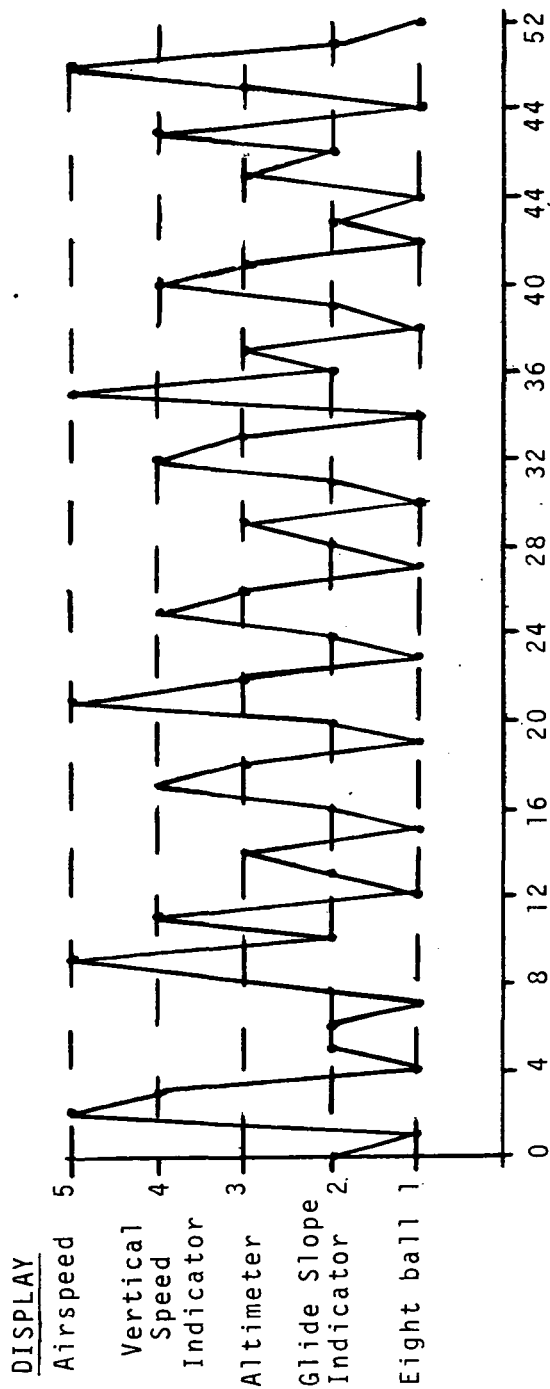
WEIGHTED STANDARD DEVIATIONS
Automatic Approach - 0 - 1 Seconds

FIGURE 13



AUTOMATIC APPROACH -- 1 - 4 Seconds

FIGURE 14-

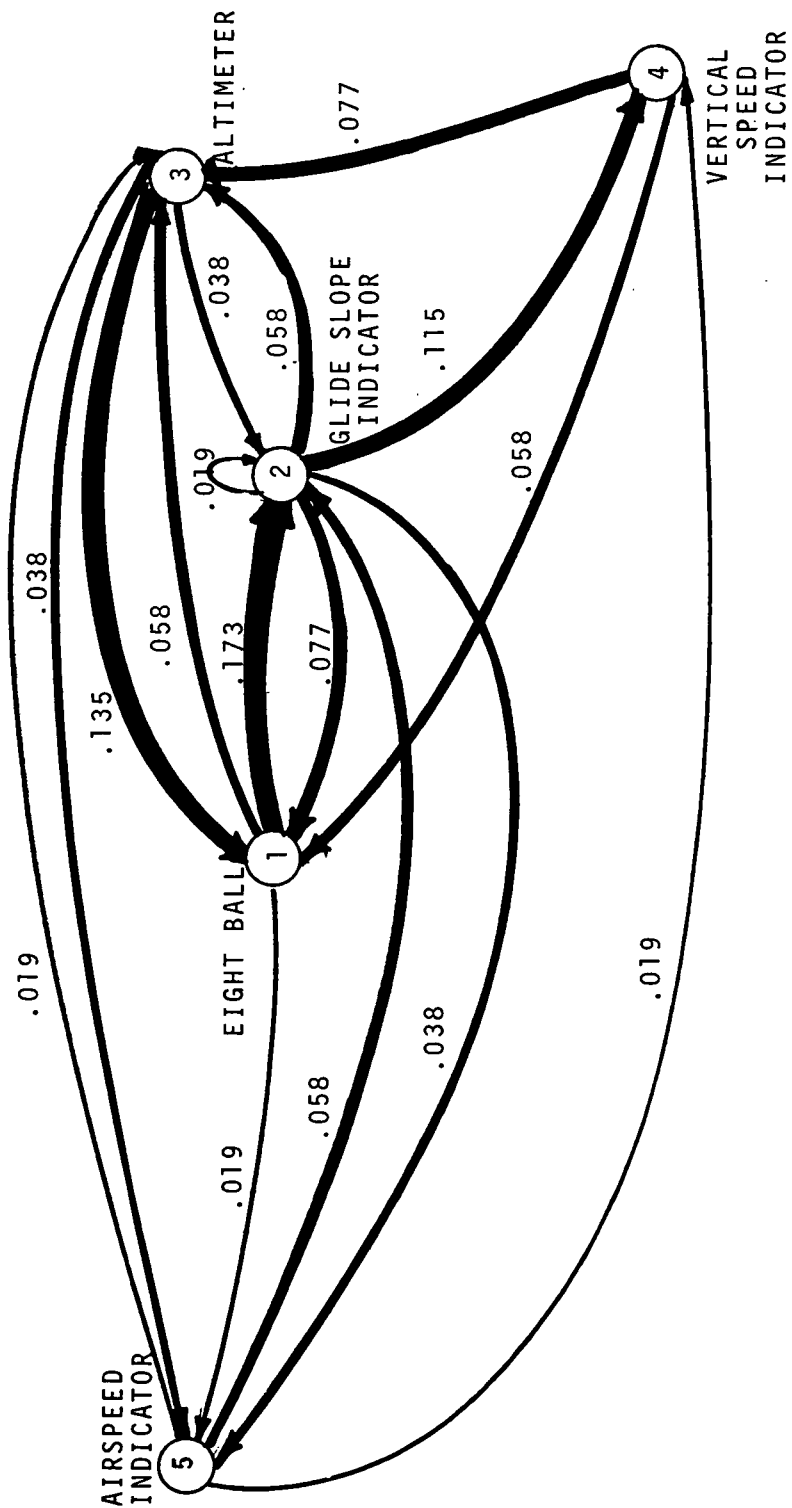


TIME STEP (1/8 Second)

LOOK-POINT PATTERN

AUTOMATIC APPROACH CONTROL

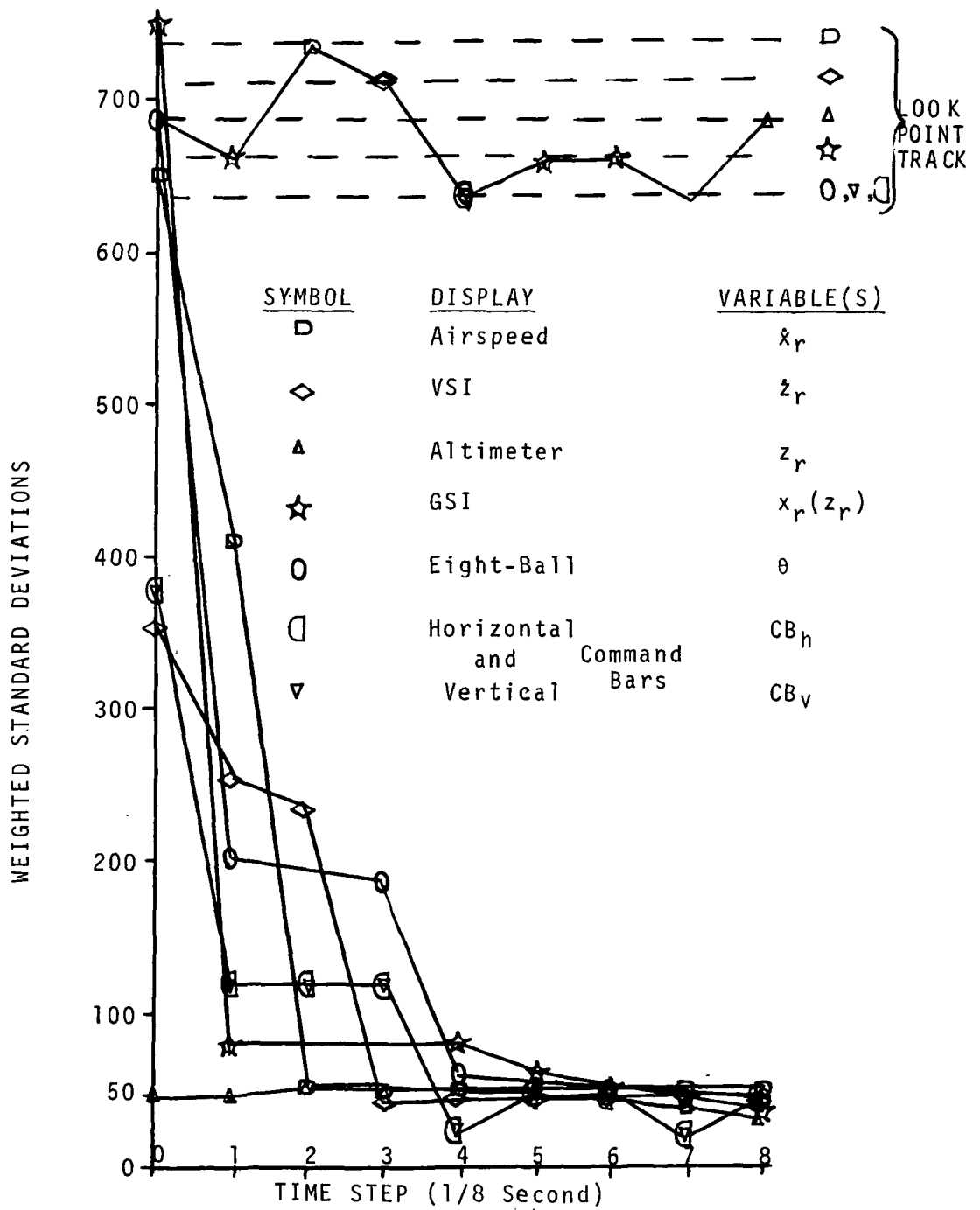
FIGURE 15



TRANSITION PROBABILITIES

Automatic Approach

FIGURE 16



WEIGHTED STANDARD DEVIATIONS
 Manual Control Approach - 0 - 1 Seconds
 FIGURE 17

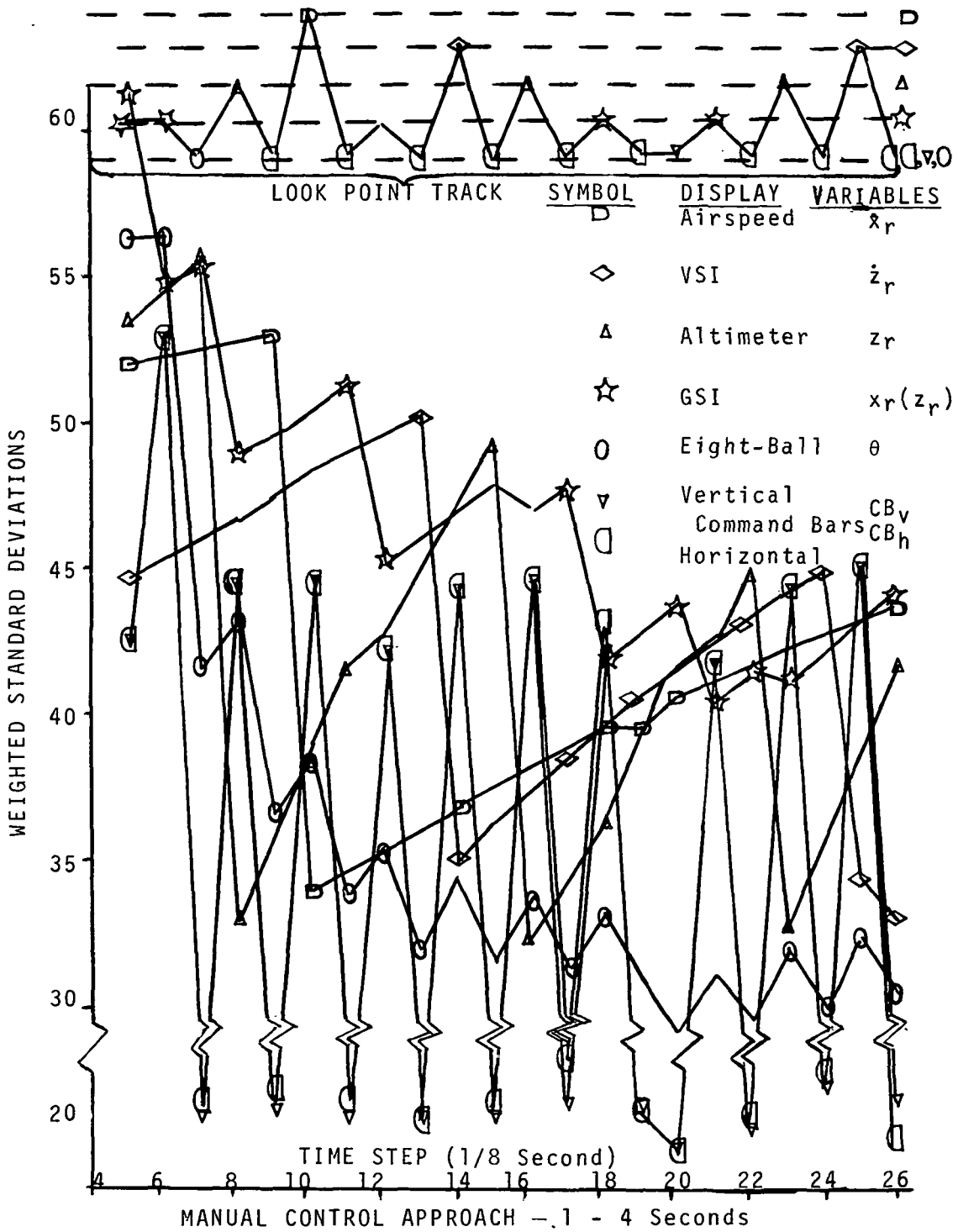
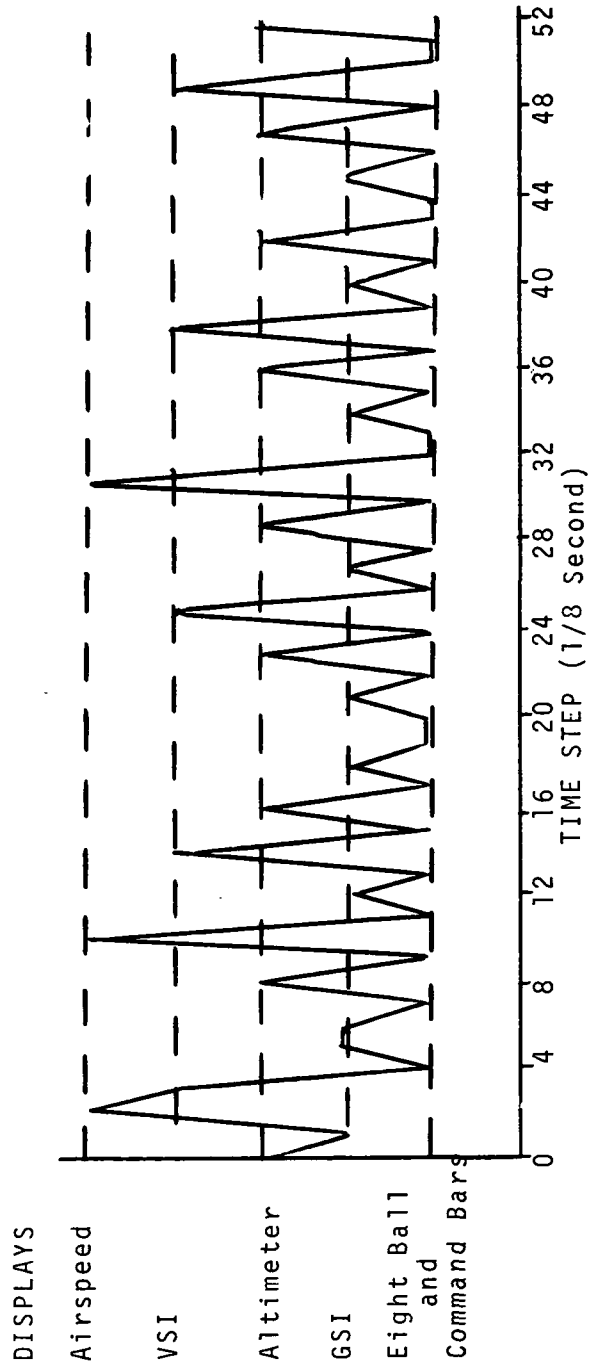


FIGURE 18



LOOK-POINT PATTERN

Manual Control Approach

FIGURE 19



TRANSITION PROBABILITIES
Manual Approach
FIGURE 20

TABLE 1
FIXED LOOK POINTS
WEIGHTED STANDARD DEVIATIONS
VARIABLES

		σ_{θ}	σ_{x_r}	σ_{z_r}	$\sigma_{\dot{x}_r}$	$\sigma_{\dot{z}_r}$
Weights		300	1	55	100	320
Time** Step	Look Point					
0	5 Airspeed	1,146	1,450	1,128	89.6	909
1	5 "	810	1,020	798	63.8	643
2	5 "	660	827	655	52.9	525
3	5 "	573	714	567	47.0	454
4	4 VSI*	519	614	451	49.3	75.5
5	4 "	480	549	388	51.5	54.7
6	4 "	447	501	345	53.6	45.8
7	4 "	423	463	315	55.6	41.0
8	2 GSI*	265	133	271	57.5	43.8
9	2 "	209	112	243	59.3	46.4
10	2 "	179	101	223	61.1	49.0
11	2 "	159	92.1	207	62.8	51.2
12	3 Altimeter	159	50.8	81.4	64.5	53.4
13	3 "	159	46.5	58.9	66.1	55.7
14	3 "	158	45.9	50.7	67.7	57.6
15	3 "	158	46.3	47.1	69.2	59.2
16	1 Eight Ball	85.5	47.1	54.5	70.7	61.1
17	1 "	66.6	47.9	61.1	72.0	63.0
18	1 "	57.6	48.6	66.6	73.4	64.6
19	1 "	52.5	49.3	71.5	74.6	66.2
20	1 "	49.5	50.0	76.5	75.9	67.8
21	1 "	47.4	50.7	80.9	77.1	69.4
22	1 "	46.2	51.3	84.7	78.3	70.7

*VSI--Vertical Speed Indicator; GSI--Glide Slope Indicator

**Time Step--1/8 second

TABLE 2
 EXAMPLE OF WEIGHTED MINI-MAX
 LOOK POINT CONTROL

Time** Step	Look Point	σ_{θ}^*300	$\sigma_{x_r}^*$	$\sigma_{z_r}^*55$	$\sigma_{x_r}^*100$	$\sigma_{z_r}^*320$
0	1 Eight Ball	102	547	836	957	688
1	5 Airspeed	104	490	671	88.8	547
2	3 Altimeter	100	350	71.5	89.9	394
3	4 VSI*	107	336	76.5	90.9	77.8
4	2 GSI*	104	73.5	80.3	91.8	78.7
5	1 Eight Ball	73.8	73.4	84.2	92.6	79.7
6	5 Airspeed	76.5	74.0	88.6	66.9	81.0
7	3 Altimeter	78.9	71.8	67.7	68.5	81.6
8	4 VSI	81.6	72.4	73.2	70.0	58.6
9	1 Eight Ball	65.7	72.2	77.6	71.4	60.5
10	3 Altimeter	68.7	71.7	61.6	72.9	62.1
11	5 Airspeed	71.7	72.3	67.7	57.4	64
12	1 Eight Ball	60.3	71.9	72.6	59.2	65.6
13	3 Altimeter	63.6	71.9	54	61.0	66.9
14	2 GSI	65.4	51.7	59.4	62.7	68.2
15	4 VSI	68.4	52.6	64.9	64.4	49.0
16	1 Eight Ball	58.5	53.2	70.4	66.0	51.5
17	3 Altimeter	62.1	53.2	52.1	67.6	53.4
18	5 Airspeed	65.1	54.1	58.9	55.3	55.7
19	1 Eight Ball	57.6	54.6	64.9	57.2	57.9
20	3 Altimeter	61.2	55.1	53.2	59.1	59.5
21	1 Eight Ball	54.3	55.6	60.0	60.8	61.4
22	3 Altimeter	58.2	56.2	53.3	62.6	63.0

*GSI--Glide Slope Indicator; VSI--Vertical Speed Indicator

**Time Step--1/8 second

TABLE 5
WEIGHTED STANDARD DEVIATIONS — MANUAL CONTROL APPROACH

Variables		θ	x_r	z_r	\dot{x}_r	\dot{z}_r	CBH*	CBV*
Rate of System Standard Dev.		.023°/sec.	25..mtrs./sec.	1.23 m/sec.	.37 m/sec.	.123 m/sec.	.18°/sec.	
Weights--W		180	1	30	50	200	29	29
Time** Step	Look Point	$W_{\theta} \sigma_{\theta}$	$W_{x_r} \sigma_{x_r}$	$W_{z_r} \sigma_{z_r}$	$W_{\dot{x}_r} \sigma_{\dot{x}_r}$	$W_{\dot{z}_r} \sigma_{\dot{z}_r}$	$W_h \sigma_h$	$W_v \sigma_v$
0	3--Alt.*	687	751	44.6	649	354	373	373
1	2--GSI*	202	79.1	46.7	410	256	120	120
2	5--Arspd*	193	79.6	49.5	51	234	120.2	120.0
3	4--VSI*	187	79.9	50.6	51.5	43	120.7	120.5
4	1--8 Ball	57.5	79.5	52.5	51.7	43.8	21.9	21.3
5	2--GSI	56.3	61.6	53.4	52.0	44.6	42.4	42.6
6	2--GSI	55.4	54.8	54.3	52.3	45.4	52.9	52.9
7	6--CBH*	41.6	55.4	55.8	52.5	46.2	20.4	19.9
8	3--Alt.	43.4	49.0	32.9	52.8	46.7	44.6	44.4
9	6--CBH	36.7	49.7	36	53	47.5	20.9	20.2
10	5--Arspd.	38.7	50.7	39	34	48.4	44.8	44.5
11	6--CBH	34.0	51.3	41.7	34.7	49	20.5	20.0
12	2--GSI	35.6	45.2	42.6	35.5	49.6	42.3	42.1
13	6-- "	32.0	46.1	45	36.1	50.2	19.9	19.9
14	4--VSI	34.4	47.1	47.1	36.9	35	44.4	44.4
15	6-- "	31.5	47.9	49.2	37.5	36.4	20.5	20.1
16	3--Alt.	33.8	47.0	31.2	38.2	37.4	44.6	44.5
17	6-- "	31.3	47.8	34.5	38.8	38.6	22.8	20.4
18	2--GSI	33.2	41.8	36.3	39.4	39.6	43.1	42.3
19	6-- "	30.7	42.8	39.3	39.5	40.6	20.0	20.2
20	7--CBV*	29.2	43.8	41.7	40.5	41.6	18.8	18.9
21	2-- "	31.2	40.4	42.45	41.1	42.4	41.7	41.7
22	6-- "	29.5	41.5	44.7	41.6	43.4	19.8	19.6
23	3-- "	31.9	41.0	32.7	42.2	44.	44.3	44.2
24	6-- "	29.9	42.1	35.7	42.7	45	21.5	21.0
25	4-- "	32.4	43.2	38.6	43.2	34.5	45.1	44.9
26	6-- "	30.4	44.2	41.4	43.7	35.8	19.6	20.4

*Alt. — Altimeter; GSI — Glide Slope Indicator; Arspd — Airspeed; VSI — Vertical Speed Indicator; CBH — Command Bar Horizontal; CBV — Command Bar Vertical.

**Time Step — 1/8 second

TABLE 6A
 TRANSITION MARIX — Manual Approach
 Eight-Ball and Command Bars Separated

DISPLAY NAME	TO FROM	D I S P L A Y N U M B E R						TOTAL "TO" TRANSITIONS	
		1	6	7	2	3	4		5
Eight-Ball Horizontal Command Bars Vertical	1	0	0	0	1	0	0	1	2
	6	0	1	1	6	5	3	1	17
	7	0	2	0	1	3	1	1	8
Glide Slope Indicator	2	0	5	3	1	0	0	1	10
Altimeter	3	0	4	3	1	0	0	0	8
Vertical Speed Indicator	4	1	4	0	0	0	0	0	5
Airspeed Indicator	5	0	1	1	0	0	1	0	3
TOTAL "FROM" TRANSITIONS		1	17	8	10	8	5	4	

TABLE 6B
 Eight-Ball and Command Bars Combined

DISPLAY NUMBER	TO FROM	D I S P L A Y N U M B E R					TOTAL "TO" TRANSITIONS
		1,6,7	2	3	4	5	
1,6,7		4	8	8	4	3	27
2		8	1	0	0	1	10
3		7	1	0	0	0	8
4		5	0	0	0	0	5
5		2	0	0	1	0	3
TOTAL "FROM" TRANSITIONS		26	10	8	5	4	

1. Report No. NASA CR-2906		2. Government Accession No.		3. Recipient's Catalog No.	
4. Title and Subtitle USE OF SENSITIVITY ANALYSIS TO PREDICT PILOT PERFORMANCE AS A FUNCTION OF DIFFERENT DISPLAYS				5. Report Date November 1977	
				6. Performing Organization Code	
7. Author(s) Michael L. Mout, George H. Burgin, and Michael J. Walsh				8. Performing Organization Report No.	
				10. Work Unit No.	
9. Performing Organization Name and Address Decision Science, Inc. 4901 Morena Boulevard San Diego, California 92117				11. Contract or Grant No. NAS1-14416	
				13. Type of Report and Period Covered Contractor Report	
12. Sponsoring Agency Name and Address National Aeronautics and Space Administration Washington, DC 20546				14. Sponsoring Agency Code	
15. Supplementary Notes Langley Technical Monitor: Patrick A. Gainer Final Report					
16. Abstract <p>A novel technique for objectively evaluating different displays by sensitivity analysis is described. First, the mathematical model used to analyze static displays is developed. The technique is based on formulating functional relationships between the state variables and the variables observable in the display (display variables). The matrix of the partial derivatives of the display variables with respect to the state variables, together with the observer's acuity function, is used to calculate expected errors in the state vector estimation.</p> <p>The technique is expanded by the use of Kalman filtering to process a time series of observation vectors. This provides a tool for analyzing displays of dynamic processes by means of a Dynamic Display Evaluation computer program.</p> <p>Results are reported using this program to simulate an Instrument Landing System approach.</p>					
17. Key Words (Suggested by Author(s)) Dynamic display evaluation, ILS simulation, Kalman filter, look-point controller, pilot performance prediction			18. Distribution Statement Unlimited - Unclassified Subject Category 60		
19. Security Classif. (of this report) Unclassified		20. Security Classif. (of this page) Unclassified		21. No. of Pages 81	22. Price* \$5.00

* For sale by the National Technical Information Service, Springfield, Virginia 22161

NASA-Langley, 1977

National Aeronautics and
Space Administration

Washington, D.C.
20546

Official Business

Penalty for Private Use, \$300

THIRD-CLASS BULK RATE

Postage and Fees Paid
National Aeronautics and
Space Administration
NASA-451



NASA

POSTMASTER: If Undeliverable (Section 158
Postal Manual) Do Not Return
